FLAVIO MASCHIETTI

TIME REVERSAL IN UWB AD-HOC NETWORKS WITH NO POWER CONTROL AND INTER-SYMBOL INTERFERENCE

MASTER'S THESIS

Advisor: Prof. Maria-Gabriella Di Benedetto
Co-Advisor: Prof. Jocelyn Fiorina

La Sapienza, University of Rome
Centrale-Supélec

School of Engineering
Department of Information Engineering, Electronics and Telecommunications (DIET)
July 13, 2015

Flavio Maschietti : *Time Reversal in UWB ad-hoc networks with no power control and inter-symbol interference,* Master's Thesis, 2015.

ACKNOWLEDGEMENTS

First and foremost, I would like to thank Prof. M.-G. Di Benedetto, who allowed me to complete my engineering studies in an international context. I had to face new challenges and problems that resulted in unexpected pleasures. I am also in debt to Prof. J. Fiorina for his valuable guidance and continuous interest which helped me throughout this final work.

I am glad to include in these lines *Adrien*, *Didier*, *Keddy* and *Marvin*, with whom I shared time and space for the whole duration of the internship. Thanks to them, I felt like home right from the start. It is together with Julien and Juliette, whom I thank for their cheerful friendship and language exchanges, that I wait for them in the *Bel Paese*.

I also wish to thank Marco and Jihane for the advice and the help - pots and pans, above all! - that they gave me in order to ease these months on French soil.

A warm hug goes to all the Roman friends, whom I've been missing during this short time *outside the walls*. I wish them nothing but the best.

Finally, I thank my parents, Sara, Davide, Leo, Nonno, and the others, for their economic and moral support, which will never cease, regardless of my choices, whatever they are.

And of course I thank K, who is always by my side - *whether near to me or far*.

Gif-sur-Yvette, May 27, 2015 F. M.

REMERCIEMENTS

Je voudrais tout d'abord remercier ma directrice de thèse, Prof. M.-G. Di Benedetto, grâce à qui j'ai pu conclure mes études dans un contexte international, lequel m'a permis de me confronter à de nouveaux défis, problèmes et plaisirs inattendus; et mon co-directeur de thèse, Prof. J. Fiorina, qui m'a guidé avec expérience, compétence et intérêt, tout au long du parcours défini.

Je suis content d'inclure dans ces lignes les personnes avec lesquelles j'ai partagé la plupart de mon temps et de mon espace pendant toute la durée du stage: *Adrien*, *Didier*, *Keddy* et *Marvin*, qui m'ont permis de me sentir comme chez moi dès le début, et que j'attends bien entendu dans le *Beau Pays* n'importe quand. La même chose s'applique également à Juliette et Julien, que je remercie pour les agréables moments passés ensemble et les amusants échanges linguistiques.

Je souhaite ensuite remercier Marco et Jihane, pour les conseils et l'assistance - mais surtout les pôeles! - qu'ils m'ont donnés afin de simplifier ces mois en terre française.

Une chaleureuse accolade aussi pour tous les amis Romains qui m'ont tendrement manqués pendant le temps que j'ai passé *hors des murs* et auxquels je souhaite le meilleur.

Enfin je remercie ma famille, donc mes parents, Sara, Davide, Leo, Nonno et les autres, pour leur soutien économique et moral, inconditionnel, quels que soient mes choix.

Et naturellement je remercie K, toujours à mes côtés - *whether near to me or far*.

Gif-sur-Yvette, le 27 mai 2015 F. M.

RINGRAZIAMENTI

Vorrei ringraziare prima di tutto la mia relatrice, la Prof.ssa M.-G. Di Benedetto, che mi ha permesso di concludere i miei studi superiori in un contesto internazionale, il quale mi ha messo di fronte a nuove sfide, problemi e gioie inaspettate; ed il mio correlatore, il Prof. J. Fiorina, che mi ha guidato con esperienza, competenza ed interesse, lungo l'intero percorso man mano delineatosi.

Sono contento di includere in queste righe i ragazzi con i quali ho condiviso spazio e tempo per l'intera durata dello stage: *Adrien*, *Didier*, *Keddy* e *Marvin*, che mi hanno fatto sentire a casa fin dal primo momento, e che attendo con gioia nel *Bel Paese*. Lo stesso vale per Juliette e Julien, che ringrazio per la spensierata amicizia ed i divertenti scambi linguistici.

Desidero poi ringraziare Marco e Jihane, per i consigli e l'assistenza - ma soprattutto le padelle! - che mi hanno fornito al fine di semplificare questi mesi in terra francese.

Un abbraccio va anche a tutti gli amici romani - direi pure milanesi, marchigiani... - dei quali ho sentito la tenera mancanza in questa breve permanenza *fuori dalle mura* e a cui auguro certamente il meglio.

Infine ringrazio la mia famiglia, dunque i miei genitori, Sara, Davide, Leo, Nonno, e tutti gli altri, per il loro supporto economico e morale, incondizionato dalle mie scelte qualunque esse siano.

E naturalmente ringrazio K, sempre al mio fianco - *whether near to me or far*.

Gif-sur-Yvette, 27 maggio 2015 F. M.

CONTENTS

LIST OF FIGURES

LIST OF TABLES

1 INTRODUCTION

Time Reversal, a prefiltering technique based on reversed channel impulse responses, can be used in UWB communications to lighten the burden on the receiver. The implementation of such precoding technique has several attractive properties.

In fact, Time Reversal can alter the statistical properties of multiuser interference. Fiorina et al., 2011, showed the influence of Time Reversal on multiuser interference in centralized networks: the focusing properties of TR make multiuser interference more impulsive, with a narrower distribution and a higher kurtosis, which lead to a performance increase.

In this work, a simulation model is presented to investigate when Time Reversal is able to increase performance in ad-hoc decentralized and uncoordinated networks.

In literature, numerous performance studies of UWB communications with Time Reversal precoding exist. Nonetheless, these studies are evaluated under strong assumptions: particular network topologies, centralized and *synchronous* communications. A comprehensive example is found in Popovski et al., 2007, where Time Reversal power controlled, *chip synchronous* transmissions are compared to conventional ones.

Often, other assumptions on the signal length are made to avoid *inter-symbol interference* and multipath dispersion. Indeed, lots of studies include a time spacing between user transmissions greater than the channel impulse response length.

All these assumptions are made to facilitate the evaluation of theoretical expressions, but lead to practical pointlessness.

Other studies such as Panaitopol, 2011, Deleuze et al., 2005, and Giancola et al., 2003, evaluated multiuser interference and its associated measures in UWB realistic scenarios, but without entering into Time Reversal details and comparisons.

In particular, Panaitopol, 2011 showed the effect of power control on multiuser interference, whereas Giancola et al., 2003 showed that multiuser interference in a UWB non-power controlled network *strongly* depends on spatial densities of the users, besides their number and bitrates.

In Deleuze et al., 2005, ISI/IFI is considered in a single user Time Hopping UWB context: a closed-form expression is given for its variance, highlighting its *non-gaussianity*.

Moreover, Ferrante, 2015, presented a discrete time model to investigate and compare robustness towards channel estimation errors both in precoded (Time Reversal) and non-precoded transmissions. The presented model, which is extended in this work, assumes a centralized *symbol-synchronous* network, where all transmission are directed to a base station, *i.e.* a common sink.

These and other studies provide a valid working basis for this work, whose principal aim is to evaluate the performance of ad-hoc UWB networks when no strong assumptions are made and both precoded and non-precoded transmissions are exploited.

In particular, a network where pairs of nodes communicate *independently* is assumed. It could represent a special kind of sensors network, suitable for UWB applications.

This restriction implies difficulties in coordinated or distributed operations. Thus, power control, *synchronization* or estimation of users channel is considered impossible.

In this scenario, Time Reversal is imperfect, leading to correlation losses and interference gain. Is it still performing well? or... Are non-precoded transmissions more robust to these limitations? This work exploits some possibilities, following a top-down approach and removing restrictions at each stage to reach a conclusion.

The following chapters are organized as follows:

IN THE SECOND CHAPTER, an introduction to UWB-IR communications is given in order to explain the elements on which the proposed framework is based.

IN THE THIRD CHAPTER, the theoretical-simulation model is elucidated. The transmitting structures and the receiving ones are explained in detail. This includes spreading and precoding matrices, thus receivers that can be adopted and the propagation channel model.

IN THE FOURTH CHAPTER, the results are presented, divided in single user and multiuser cases. The performance is evaluated in terms of *mutual information*, thus *spectral efficiency* and *bitrate* when *Gaussian* inputs are used. While the BER - *i.e.* bit error ratio - is the common performance measure adopted when inputs are assumed to be *binary*.

IN THE FIFTH CHAPTER, final conclusions and possible future investigations are reported.

IN THE APPENDIX, useful mathematical fundamentals are described. In addition, the MATLAB code of the entire model is shown.

2 AN OVERVIEW OF UWB-IR COMMUNICATION SYSTEMS

Contents

Ultra-wideband (UWB) is a wireless communication method for transmitting information over a large bandwidth. Such a large bandwidth offers advantages concerning signal robustness, information transfer rate, implementation easiness, but leads also to fundamental differences from conventional narrowband schemes. This chapter aims to outline these techniques, which have experienced an increasing interest from chip manufacturing companies, standardization agencies and research institutes in the last decade.

2.1 UWB BASICS

A signal is said to be UWB if its bandwidth is higher in respect to the center frequency, *i.e.* its *fractional bandwidth* is high:

$$FB = \frac{f_H - f_L}{\frac{1}{2}(f_H + F_L)} \tag{2.1.1}$$

In particular, the Federal Communications Commitee (FCC) gives the following definitions:

- 10 dB fractional bandwidth higher than 0.20;
- Spectral occupation higher than 500 MHz.

It is natural that the utilization of such an ultra-wideband must be regulated in order to not disturb the transmissions of emitters who own the rights to use the portions of electromagnetic spectrum assigned to them.

2.1.1 FCC Regulations

Several measurements campaigns were performed in the United States in order to verify the possibility for UWB systems to coexist with other existing systems: a final report was released in 2001.

In 2002, the FCC approved the first guidelines allowing the intentional emission of UWB signals and specified emission masks.

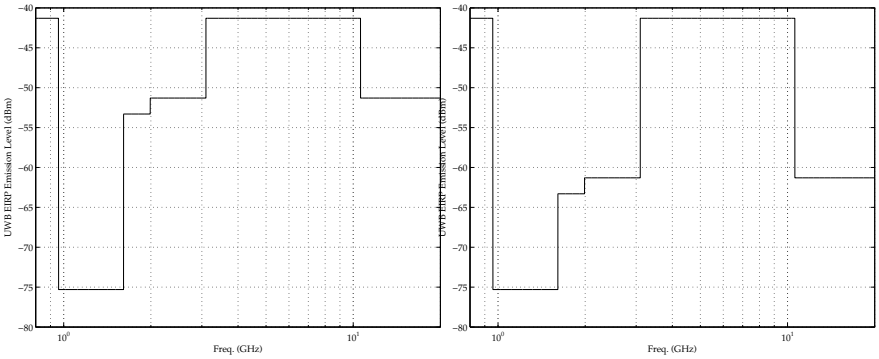

Figure 2.1-1: FCC emission masks for indoor and outdoor propagation.

According to the FCC regulations, a signal is UWB if its fractional bandwidth is higher than 0.2 or if its spectral occupation is higher than 500 MHz; this definition creates a threshold at 2.5 GHz:

- Under the threshold the signals are UWB if their fractional bandwidth is higher than 0.2;
- Above the threshold the signals are UWB if their spectral occupation is higher than 500 MHz.

Indeed, consider a signal with bandwidth between 20 and 22 GHz: this signal is UWB due to its spectral occupation of 2 GHz. However, it has a fractional bandwidth equal to:

$$\mathrm{FB} = \frac{2 \times 10^9}{21 \times 10^9} \simeq 0.09 < 0.2 \tag{2.1.2}$$

Table 1: FCC radiation limits for indoor and outdoor propagation.

Frequency	Indoor EIRP (dBm/MHz)	Outdoor EIRP (dBm/MHz)
$0-960$	-41.3	-41.3
$960-1610$	-75.3	-75.3
$1610-1990$	-53.3	-63.3
$1990-3100$	-51.3	-61.3
$3100-10600$	-41.3	-41.3
Above 10600	-51.3	-61.3

2.2 GENERATION OF UWB SIGNALS

There are several procedures to obtain a UWB signal. In the impulse radio case (IR) the concept is simple: short (in time) pulses, which bring data, are radiated from the transmitter to the receiver.

These pulses determine the bandwidth of the signal. In order to operate in the $3.1-10.6$ GHz band, which is the most interesting spectrum portion in the FCC mask, a pulse width of about 5×10^{-11} s should be used.

This kind of transmission does not require the use of additional carrier modulation as the pulse will propagate well in the radio channel.

PPM and PAM are *commonly* adopted modulation techniques. In addition to modulation and in order to shape the spectrum of the generated signal, information data is encoded using pseudorandom or pseudonoise codes.

In this work, Time Hopping (TH) is used: the following equations are written for such encoding technique.

It is important to remember that a UWB signal is not limited to IR signals: if a signal respects the FCC definitions of spectral occupation and fractional bandwidth, it is still UWB.

2.2.1 Generation of TH-UWB Signals

When Time Hopping is used, the encoded data introduces a *time dither* on the generated pulses. The following is the general block diagram for this transmission technique, when PAM is used as modulation scheme.

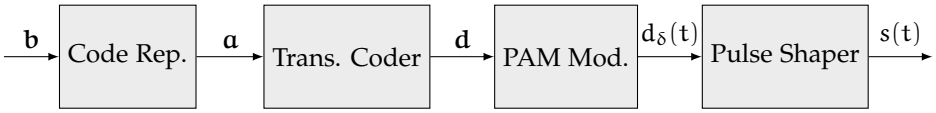

Figure 2.2-2: Transmission chain for a PAM-TH-UWB signal.

1) The *Code Repetition Coder* takes in input a sequence $\mathbf{b}$ generated at a rate $R_b = {}^1/_{T_b}$ bits per second and generates a sequence $\mathbf{a}$ where each bit of the input sequence is repeated N_s times: the output sequence has thus a rate of $R_c = {}^{N_s}/_{T_b} = {}^1/_{T_s}$. This block introduces *redundancy* and is denoted as $(N_s, 1)$ code repetition coder. After that, the sequence $\mathbf{a}$ is transformed to an antipodal one.

2) The *Transmission Coder* applies an integer-valued code $\mathbf{c}$, *i.e.* the TH code, to the sequence $\mathbf{a}$ and generates a new sequence $\mathbf{d}$. The generic element of the sequence $\mathbf{d}$ is thus expressed as $d_i = c_i T_c$ where T_c is called *chip time*. The chip time is a constant term and it satisfies the condition $c_i T_c < T_s$ for all c_i.

3) The *PAM Modulator* takes in input the sequence $\mathbf{d}$ and generates a sequence of mathematical pulses $\mathbf{d}_\delta$ at a rate ${}^1/_{T_s}$.

4) The *Pulse Shaper* shapes the pulses in input with its impulse response $p(t)$. This impulse response must be such that the signal at the output of the pulse shaper filter is a sequence of non-overlapping pulses.

Moreover, pulse shaping is needed to adjust the PSD of the emitted signal in order to meet the limitations seen in section 2.1.1. In general, a second Gaussian derivative is adopted.

The complete expression for a PAM-TH-UWB signal is thus given as:

$$s(t) = \sum_{i=-\infty}^{+\infty} a_i p(t - iT_s - c_i T_c) \tag{2.2.1}$$

Using PPM along with Time Hopping does not *drastically* change the transmission scheme: in this case, the sequence $\mathbf{a}$ is not transformed to an antipodal one and there is a PPM modulator which utilises the code a_i to control the position of the pulses, not the amplitude:

$$s(t) = \sum_{i=-\infty}^{+\infty} p(t - iT_s - c_i T_c - a_i \epsilon) \tag{2.2.2}$$

where ϵ is called *PPM shift* and T_s is the frame time.

Another technique called Direct Sequence (DS) can be used to encode UWB signals. In DS-UWB, no time dither is introduced: signals are encoded using a *pseudorandom* sequence, which makes them noise-like.

Therefore, the pulses are transmitted *continuously*, whereas in TH-UWB, a pseudorandom sequence defines the chips where the pulses are transmitted.

In Figure 2.2-3, a comparison between TH and DS is shown.

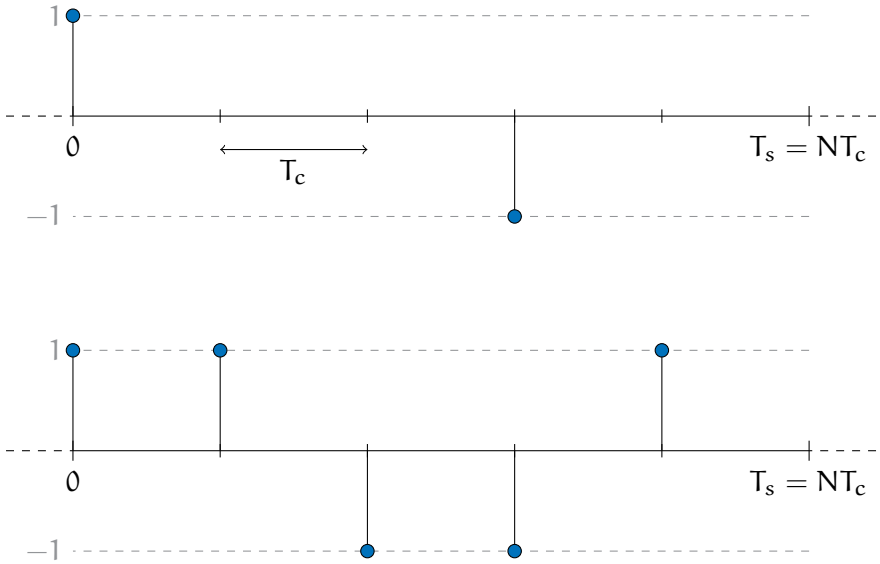

Figure 2.2-3: TH vs DS time axis structure with $N = 5$.

In particular, a frame of duration T_s is divided in $N = 5$ chips of duration T_c. In this scheme, which refers to the transmission of a positive bit, the TH sequence and the DS one are as follows:

$$\mathbf{x}_{TH} = [1\ 0\ 0\ -1\ 0] \tag{2.2.3}$$

$$\mathbf{x}_{DS} = [1\ 1\ -1\ -1\ 1] \tag{2.2.4}$$

In fact, Time Hopping can reduce to Direct Sequence when all elements in $\mathbf{x}_{TH}$ are non-zero: in this work, TH codes are assumed to have just one non-zero element, which can be either positive or negative.

2.2.2 Time Hopping Multiple Access

The impulse radio technique is based on the transmission of short pulses. This technique has several particular and attractive properties.

However, an important problem has to be outlined. Consider a scenario where several users are sharing the radio resource: collisions between pulses can occur. This cause the signal-to-interference ratio (SIR) to become inacceptable, leading to a high bit error ratio (BER).

The nature of Time Hopping makes it easier to define a multiple access scheme for a multiuser environment. In fact, a different TH code can be assigned to each user in the UWB network, allowing their signals to not superimpose.

The same can happen with a DS encoding, although in this case there is no separation in time and the *orthogonality* between users is related to that of DS sequences.

The collisions are still possible, but the code repetition coder could represents each data bit with several short pulses. Thus, even if one pulse collides with a signal from another user, other pulses in the sequence will *probably* not.

Increasing the number of pulses per bit decrease the significance of one collision but increase *redundancy*.

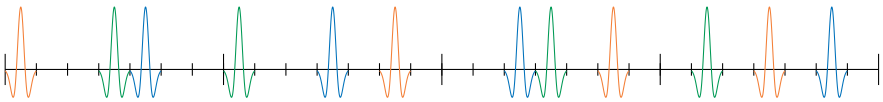

Figure 2.2-4: TH Multiple Access scheme with $N = 7$ and $K = 3$ users in a *synchronous* environment.

2.3 RECEIVER STRUCTURES FOR UWB SIGNALS

The main problem of receiver design is to find the optimal approach to extract the useful signal from the received one.

When considering propagation over an AWGN channel, thermal noise is the *only* source which corrupts the useful signal:

$$r(t) = r_u(t) + n(t) = \alpha s(t - \tau) + n(t) \tag{2.3.1}$$

where α is called *channel gain* and $\tau = {}^{D}/_{c}$ *channel delay*, while $n(t)$ is a realization of a random Gaussian process with a PSD equal to $\mathcal{N}_0/2$.

In these channels, a PAM-TH-UWB signal is received as follows:

$$r(t) = \sum_{i=-\infty}^{+\infty} a_i \sqrt{\alpha^2 E_{TX}} p_0(t - iT_s - c_i T_c - \tau) + n(t) \tag{2.3.2}$$

where $\alpha^2 E_{TX} = E_{RX}$ is the received *energy per pulse* and $p_0(t)$ is the normalized pulse.

The effect of the thermal noise is to distort the waveform of the transmitted pulses: the amount of distortion depends on the ratio between the useful energy E_{RX} and the noise PSD $\mathcal{N}_0$, that is, the signal-to-noise ratio (SNR).

As known, the optimum receiver for an AWGN channel is the one which chooses for the waveform more correlated to the received one. There can be M possible waveform, depending on the constellation.

2.3.1 UWB Multipath Receivers

The AWGN channel is modeled after two parameters. In this case, the receiver structure is *relatively* simple. In the presence of multipath - *i.e.* in the real radio propagation - both the channel model and the receiver become more complex. Moreover, the channel exhibits time-variant characteristics.

In these cases, the received signal is expressed as follows:

$$r(t) = \sum_{n=1}^{N(t)} a_n(t)p(t-\tau_n(t)) + n(t) \tag{2.3.3}$$

where $a_n(t)$ and $\tau_n(t)$ are the gain and the *delay* of the channel for each multipath replica n in function of time, while $N(t)$ is the number of different paths observed in time.

Introducing the impulse response $h(t)$ of the channel, the received signal can be also expressed as follows:

$$\begin{aligned} r(t) &= s(t) * h(t) + n(t) \\ \text{where } h(t) &= \sum_{n=1}^{N(t)} a_n(t)\delta(t-\tau_n(t)) \end{aligned} \tag{2.3.4}$$

It is possible to assume that the variation rate of the impulse response's parameters is low compared to the transmission rate: in other words, the channel is assumed to be *stationary* in an observation interval T.

The replicas of the received signal are overlapping if their inter-arrival time is lower than the duration of the pulse: in this case, the signals associated to the different paths are somewhat correlated.

In UWB-IR communications, the pulse width does not get above fractions of nanoseconds: it is possible to assume a total absence of correlated signals at the receiver.

UWB-IR receivers can thus combine a great number of indipendent replicas, associated to the same pulse.

There exist different techniques:

- *Selection Diversity* (SD): the receiver selects the best replica in terms of SNR and makes the decision on this replica;
- *Equal Gain Combining* (EGC): the receiver aligns in time all the replicas and then sum them without particular weights;
- *Maximal Ratio Combining* (MRC): the receiver aligns in time all the replicas and then makes an SNR-based sum.

In these cases, the receiver increases performance *only* if each replica can be *separately* resolved: as a consequence, it is not possible to use the AWGN optimum receiver.

Indeed, the optimum receiver must include additional correlators, associated with the various replicas of the transmitted waveform: such a receiver is called Rake.

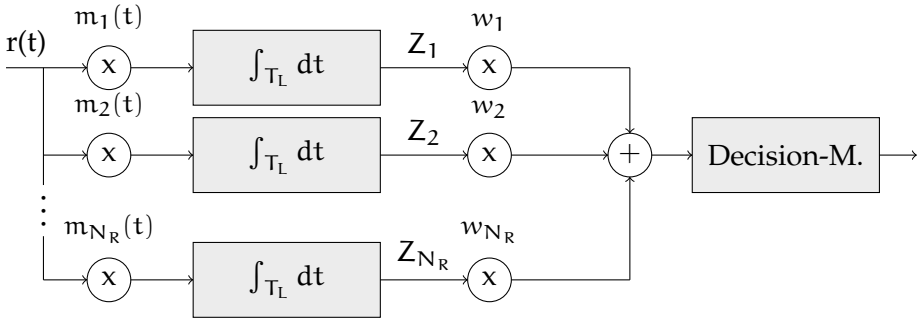

Figure 2.3-5: Rake receiver with N_R parallel correlators.

N_R correlators form the Rake receiver, each of them matched with a certain replica of the transmitted signal:

$$m_i(t) = m(t - \tau_i) \tag{2.3.5}$$

Thus, the Rake receiver must be able to resolve and update the channel's impulse response. For this reason, channel state informations (CSI) are often evaluated at the receiver.

According to the sum technique, weights w_i are used after the correlation: with SD, the weights are equal to zero except that for the chosen replica; with EGC, the weights are all equal to one, while with MRC are proportional to the amplitude of the signal.

An equivalent scheme use a single correlation mask $m(t)$ along with the insertion of a *delay block* in each line.

Along with this scheme, the receiver must know the time distribution for each of the contributions due to multipath.

In severe multipath environments, Rake receivers might require a large number of fingers. As such, implementing a Rake receiver might be cost-ineffective. Several strategies, which are summerized in Table 2, can be used to decrease its *complexity*.

Table 2: Rake receiver variations.

Receiver	Fingers/Replicas
All-Rake	All replicas
Partial Rake	First L replicas
Selective Rake	Best L replicas

2.3.2 Time-Reversal UWB Communications

In multipath channels - as seen - the received signal is not a single and clean pulse $p(t)$:

$$g(t) = \sum_{i=1}^{L} \gamma_i p(t - \tau_i) \tag{2.3.6}$$

where γ_i and τ_i are the amplitude and the *delay* associated with the i-th path and L is the number of paths.

In these cases, the free-space propagation receiver is not optimal: the receiver is called *one finger Rake* (1-Rake) and it collects the energy of a single path.

In order to harvest enough of the energy distributed in the entire impulse response, Rake receivers with at least 10 fingers must be designed, as it can be seen on Table 3. Such a design is not low cost.

In the best case, the receiver has to be adapted to the entire received waveform. The following correlation mask is used:

$$m(t) = \sum_{n=0}^{N_s-1} g_0(t - nT_s - c_n T_c) \tag{2.3.7}$$

The receiver which implements this correlation mask is called *all-Rake*.

Nothing new... What is Time Reversal? This is a technique experimented in acoustics and ultrasound contexts but which fits well also for UWB communications.

The All-Rake receiver correlates the received signal with the pulse convolved with the impulse response of the multipath channel: the principle of *Time Reversal* consists of switching the *complexity* from the receiver to the transmitter. A convolution with the reversed channel is made at the transmitter side. It is a *pre-filtering*.

Advantages of Time Reversal are also temporal and spatial focusing, properties which are highlighted in Figure 2.3-6.

The prefilter accentuates the strongest path. In fact, the resulting impulse response to which a signal is subjected to is the autocorrelation of the channel, which is an even function with a peak in the center.

In this case, a classic *one finger* receiver, aligned to the peak, can be used. So, Time Reversal makes possible to use a simple receiver in rich multipath environments.

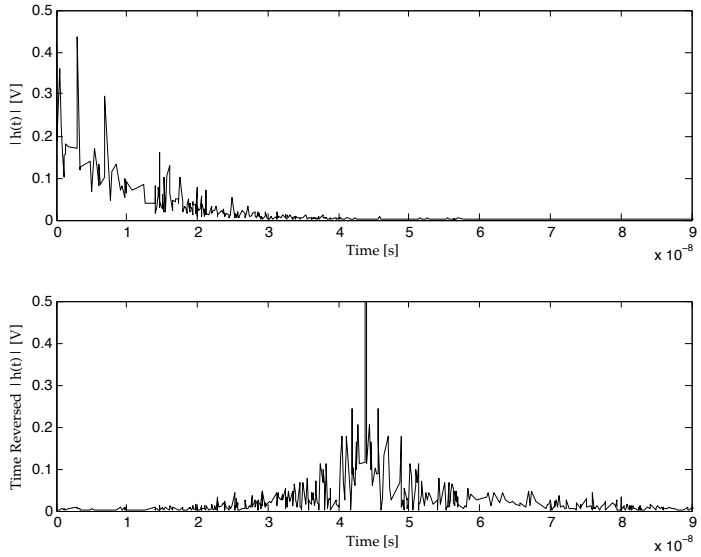

Figure 2.3-6: Impulse response of a UWB channel $h(t)$ and overall response after pre-filtering $h(-t) * h(t)$.

Table 3: *Energy efficacy* of the chain as a function of N_{in} and N_{out}.

N_{out}	$N_{in} = 1$	$N_{in} = 10$	$N_{in} = 20$	$N_{in} = All$
1	14.8%	54.5%	75%	100%
10	55%	81.8%	98.8%	120.3%
20	75.2%	94%	112.1%	132.4%
All	100%	144.2%	165.2%	191.6%

In Table 3, the percentage of *energy per pulse* captured in reception, is shown in terms of numbers of fingers N_{in} at the transmitter side, and N_{out} at the receiver side.

Is it better to use a *one finger* receiver or an *all-Rake* one? The *one finger* receiver used in time reversed environments has the same performance - in terms of noise robustness - of an All-Rake without Time Reversal: the two schemes collect the same amount of energy.

However, an All-Rake receiver *always* collects more energy than a *one finger* receiver and thus it has *always* better performance.

When using Time Reversal, the All-Rake receiver has to be adapted to $p(t) * h(-t) * h(t)$ so the paths are those of $h(-t) * h(t)$ and not those of $h(t)$.

Time Reversal can be reduced to a *partial* TR, *i.e.* $N_{in} \neq$ All: pre-filtering is made with an impulse response $h^*(t)$ which containts a subset of the paths of $h(t)$. In this case, the receiver must be adapted to $p(t) * h^*(t) * h(t)$.

In this work, four schemes/receivers are evaluated:

- 1-Rake: $N_{in} = N_{out} = 1$
- All-Rake: $N_{in} = 1$, $N_{out} =$ All
- TR 1-Rake: $N_{in} =$ All, $N_{out} = 1$
- TR All-Rake: $N_{in} = N_{out} =$ All

2.3.3 Multiuser UWB Communications

When several users share the radio resource in a UWB network, an other element that limits the performance of the Rake receiver appears: the *multiuser* interference.

Referring to the scheme in Figure 2.3-7, when K users are active, the received signal for the user 1 can be written as:

$$r_1(t) = s_1(t) * h_1(t) + \sum_{k=2}^{K} s_k(t) * h_k(t) + n(t) \qquad (2.3.8)$$

where the second term in the RHS is the multiuser interference.

Multiuser interference - *i.e.* x_{mui} - depends on a multitude of factors: encoding technique, number of users in the network, channel characteristics, adopted pulse, *etc*.

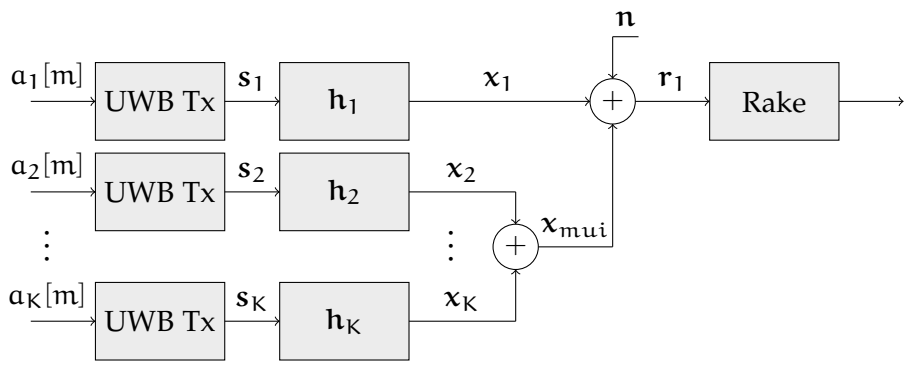

Figure 2.3-7: General scheme for a UWB multiuser environment.

Modeling multiuser interference is crucial in the design of wireless networks. In impulse radio networks, most of the adopted models are based on classical spread spectrum communications like CDMA, which do not address specific features for IR networks, where spectrum spreading is due to the radiation of short time-limited pulses.

In order to ease things, a *standard Gaussian approximation* (SGA) is often assumed: MUI is modelled as a Gaussian random process, just like thermal noise. In this case, a theoretical evaluation of BER is straightforward.

In UWB communications, this approximation leads however to an optimistic estimate of the overall interference: it can be shown that SGA gives good approximations as the number of interfering users increase; a behavior that could be explained in central limit theorem situations.

Another successful method capable to evaluate and to shape MUI analyses the collisions occurring between pulses belonging to different transmissions: in fact, in impulse radio communications, the interference at the receiver is due to this phenomenon.

Impact of Time Reversal on the Multiuser Interference

It can be shown that Time Reversal makes the multiuser interference more impulsive under certain scenarios.

Experiments showed that the *kurtosis* increases as the number of paths considered from $h^*(t)$ increase.

In this work, Time Reversal is *always* made considering the entire impulse response, *i.e.* $N_{in} = \text{All}$.

Trade-offs between the number of fingers in transmission and reception are possible, although no further investigations are made here.

The increase of kurtosis can improve performance.

2.4 UWB ADVANTAGES AND DISADVANTAGES

This chapter can be concluded with an overview of the major advantages and disadvantages of UWB communications.

Important benefits that UWB offers are:

- It provides a large absolute bandwidth which allows transmissions at high data rates (above 100 Mbit/s) over short distances (less than 10 m). This bandwidth also creates high resilience to fading: the different spectral components of the signal encounter different propagation conditions. Thus, there is a high prob. that at least some of them can penetrate obstacles or otherwise arrive to the receiver. In other words, the signal is more robust to shadowing effects;

- Multiuser interference can be much reduced in UWB communications, allowing a large number of terminals to share the radio resource;

- It tolerates well multipath channels. The use of short pulses creates non-overlapping signal sequences which do not increase interference. Moreover, multipath can increase the performance of a UWB radio link: the Rake receiver can collect several replicas from the multipath channel;

- Using short pulses, it can provide accurate range informations, leading to radar, geolocation and imaging applications;

- It has potentially low complexity and low cost due to its baseband nature. The UWB transmitters produce pulses which are able to propagate without the need for an additional RF mixing stage, *i.e.* UWB transmission is carrier less. This means that UWB does not require local oscillators and their associated phase tracking loops. Thus, UWB schemes can be implemented in low-cost, low-power integrated circuit processes.

With the above discussed advantages, UWB provides useful wireless communication applications: computer peripherals networks (wireless USB), sensors networks (medical, automotive, *etc*) and positioning systems above all.

Some limitations that must be somehow overcome are:

- UWB signals needs high-speed ADCs and high-speed DSPs to be processed; moreover, UWB receivers are subject to long synchronization times and must be complex enough to handle multipath channels: still, the channel characterization is not trivial due to wide bandwidth and reduced signal power;
- It requires wideband antennas; these antennas are more bigger and more expensive than narrowband antennas: there is an electrical engineering challenge on this topic;
- Lack of common standards between industries;
- Limitations in range due to the FCC emission masks: the low output power - crucial in order to avoid interference to other radio technologies - leads to smaller coverage area; with regular antennas, *i.e* non high gain, the range of UWB signals is from 10 to 20 m.

3 A DISCRETE TIME MODEL FOR UWB-IR COMMUNICATIONS

Contents

The nature of impulse radio communications allows to model the entire communication scheme described in chapter 2 with a *discrete time* model. This core chapter aims to present this model and to outline all its components.

3.1 OVERVIEW OF THE DISCRETE TIME MODEL

An ad-hoc network where K pairs communicate in an uncoordinated manner, *independently* from each other, is considered. A transmitter and a receiver form each pair, leading to the so-called *point-to-point* model. Then, a *reference* pair is chosen to evaluate the performance of the entire network.

3.1.1 Network Characterization

One point in $\mathbb{R}^2$ represents each node, *i.e.* a transmitter or a receiver, whose position is decided according to a uniform distribution with variable interval.

Important parameters of the network are thus:

- K = number of pairs;
- N = number of chips in a frame;
- K/N = load of the network.

As the number of pairs is fixed, the *load* K is quite important since it correlates the number of chips in a frame with the number of pairs in the network. For example, when Load $= 1$, the number of chips in a frame is equal to the number of pairs in the network.

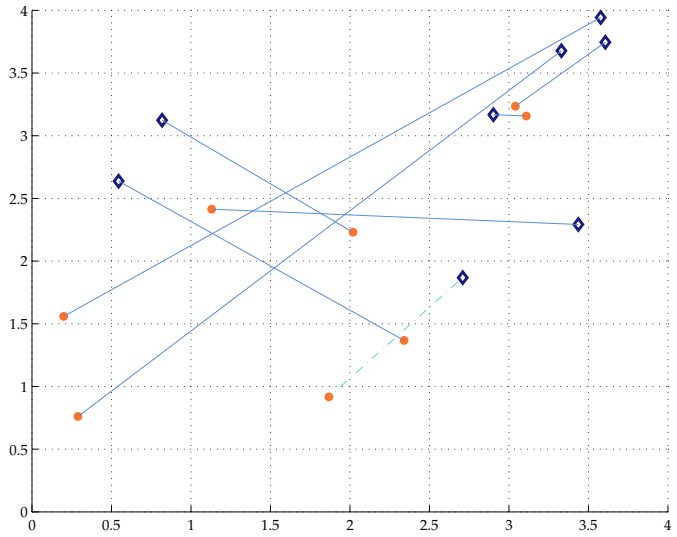

Figure 3.1-1: A sample scenario generated when $K = 8$ (16 nodes).

Figure 3.1-1 shows a sample scenario of the ad-hoc network. The paler dashed line denotes the reference pair/link. All transmissions are considered to be omnidirectional.

A generic transmitter emits data, which is encoded into a sequence of information bearing symbols b_n. Considering just one frame - *i.e.* a fixed n - the transmitted signal when no prefiltering is used is:

$$x(t) = b_n \sqrt{E_x} p(t - nT_s - mT_c) \tag{3.1.1}$$

where T_s is the frame period, T_c is the chip time and $p(t)$ is the waveform associated with the m-th symbol of the generic user. E_x is the transmitted *energy*, which will be consider equal to 1 in the following expressions.

In general, $p(t)$ is a spread-spectrum signal and has band $[-W/2, W/2]$, *i.e.* its spectrum is zero for $|f| > W/2$.

The transmitted signal $x_k(t)$ of each user propagates over a multipath channel with impulse response $h_k(t)$, which distorts the signal.

The received signal - at the generic demodulator - is:

$$y(t) = \sum_{k=1}^{K} x_k(t) * h_k(t) + n(t) \tag{3.1.2}$$

where $n(t)$ is a white Gaussian noise with PSD $^{\mathcal{N}_0}/_2$ ($^{W}/_{Hz}$).

The demodulator for user k estimates its symbols by considering users $j \neq k$ as unknown interference over user k.

In the adopted model, the receiver is a single user detector, which does not take in account a joint multiuser detection.

3.1.2 Single User Channel

In order to facilitate the comprehension of the multiuser case, it is useful, as a first step, to describe the single user one.

If the transmission does not foresee prefiltering and a single b - *i.e.* one frame - is emitted, the received signal is:

$$y(t) = x(t) + n(t) = b \sum_{k=0}^{N-1} s[k]p(t - kT_c) * h(t) + n(t) \tag{3.1.3}$$

where the *spreading* sequence $\mathbf{s} = (s[0], \ldots, s[N-1])^T$ is made explicit and $p(t)$ is a zero-excess bandwidth normalized pulse with bandwidth W. Assuming $T_c = {}^1/_W$, the equation (3.1.3) is rewritten as:

$$y(t) = b \sum_{k=0}^{N-1} s[k] \sum_{l=0}^{L} h[l]p(t - (l+k)/W) + n(t) \tag{3.1.4}$$

that follows also from $p(t)$ - and therefore $p(t) * h(t)$ - being bandlimited to $^W/_2$. This is just another way to write equation (2.3.4).

The spreading sequence - as said in section 2.2 - is a Time Hopping code, for which all $s[k]$ are zero, except one. Hence, $\|\mathbf{s}\|^2 = 1$.

Interframe Interference

In the single user case, one would expect to find just a single source of noise, *i.e.* thermal noise. In general - in impulse radio UWB communications above all - this is not true.

Since the time axis is divided in frames, when a channel introduces multipath, it can be possible to find some replicas in the successive frames. In fact, this is not uncommon.

A UWB channel has a time spread of about $50 - 100$ ns; considering that a frame lasts for NT_c ns, where $T_c < 10$ ns, it is plausible to have frames-overlapping replicas, which originate *interframe interference*.

In TH-UWB communications, ISI (*inter-symbol interference*) and IFI (*interframe interference*) are interchangeable terms. When a signal in a frame n overlaps a signal in a frame m, it creates both IFI and ISI: indeed, each frame contains a *symbol*.

An example scheme is depicted in Figure 3.1-2, where some replicas of the pulse emitted in the first frame - highlighted in red - arrive at the receiver in the successive frames.

It is not hard to find in literature the assumption of high enough frame lengths or guard times to avoid interframe interference: that works, although with a high price in terms of bitrate.

In other cases, interframe interference must be taken into account, or removed, if possible.

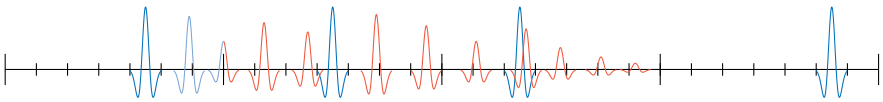

Figure 3.1-2: Transmission scheme with $N = 7$ and interframe interference.

The Discrete Model

The equivalent discrete model is obtained when equation (3.1.4) is projected onto $\{p(t - {}^{k}/_{W}) : k = 0, \dots, (N + L - 1)\}$:

$$\mathbf{y} = \mathbf{C}\mathbf{x}b + \mathbf{n} \tag{3.1.5}$$

where $\mathbf{C}$ is a convolution matrix with dimensions $(N + L) \times N$, having assumed $h[l] = 0$ for $l < 0$, and $h[l] = 0$ for $l > L = {}^{T_d}/_{T_c}$. T_d is the finite *time spread* of the UWB channel.

In general, when prefiltering is adopted - with prefiltering impulse response $h_p(t)$ - the equation (3.1.5) generalizes to:

$$\mathbf{y} = \mathbf{C}\mathbf{P}\mathbf{x}b + \mathbf{n} \tag{3.1.6}$$

where $\mathbf{P}$ is a convolution matrix with dimensions $(N + 2L) \times (N + L)$ and where $\mathbf{n}$ includes both thermal noise and interframe interference, with the latter arising from previous frames.

In this work, the channel used in simulations is a discretized version of the IEEE 802.15.3a, described in section 3.4, while Time Reversal is used as prefiltering technique.

Receiver structure

In the case of equation (3.1.5), the conventional optimal receiver is a matched filter, *i.e.* an All-Rake receiver when a multipath channel is considered. Knowing the spreading sequence $\mathbf{x}$ and the channel matrix $\mathbf{C}$, a valid statistic for b is obtained as:

$$z^{AR} = \frac{\mathbf{C}\mathbf{x}^T}{\|\mathbf{C}\mathbf{x}\|}\mathbf{y} = \frac{\mathbf{C}\mathbf{x}^T}{\|\mathbf{C}\mathbf{x}\|}(\mathbf{C}\mathbf{x}b + \mathbf{n}) \tag{3.1.7}$$

When prefiltering is adopted, the receiver is a 1-Rake receiver matched on the overall impulse response:

$$z^{TR} = \boldsymbol{e}_{L+j_x}^T\mathbf{y} = \boldsymbol{e}_{L+j_x}^T\mathbf{C}\mathbf{P}\mathbf{x}b + \boldsymbol{e}_{L+j_x}^T\mathbf{n} \tag{3.1.8}$$

where $\boldsymbol{e}_{L+j_x}^T$ denotes the canonical vector with a one in the $L+j_x$ coordinate, *i.e* the peak in the time reversed impulse response. In fact, an additional shift is required to align the correlator with the peak in the received signal of the reference transmitter. The number j_x depends on the time hopping code.

As said in section 2.3.2, also an All-Rake receiver - matched on the overall impulse response - can be used along with time reversal; it leads to the following decision variable:

$$z^{TR} = \frac{(\mathbf{C}\mathbf{P}\mathbf{x})^T}{\|\mathbf{C}\mathbf{P}\mathbf{x}\|}\mathbf{y} = \frac{(\mathbf{C}\mathbf{P}\mathbf{x})^T}{\|\mathbf{C}\mathbf{P}\mathbf{x}\|}(\mathbf{C}\mathbf{P}\mathbf{x}b + \mathbf{n}) \tag{3.1.9}$$

As well-known, in a single user scenario, there is no performance difference between an All-Rake receiver and a TR 1-Rake one.

3.1.3 Multiuser Channel

The direct extension of equation (3.1.6) to K transmitters is as follows:

$$\mathbf{y} = \sum_{k=1}^{K} \mathbf{C}_k\mathbf{P}_k\mathbf{x}_k b_k + \mathbf{n} \tag{3.1.10}$$

where $\mathbf{C}_k$ and $\mathbf{P}_k$ are the channel and the precoding convolution matrices for the user k, with same dimensions as in equation (3.1.6).

This extension is valid under the assumption that all transmitters are *symbol-synchronous*. In the considered scenario, this assumption is not reasonable: the transmitters communicate with their associated receiver without a distributed link setup phase or a control signal.

In simulations, this assumption is indeed not considered: users are *randomly* shifted in time.

Hereinafter, the assumption is nevertheless kept in order to lighten notation.

Receiver structure

In the multiuser case, the receivers are equivalent to those seen for the single user case. Without prefiltering, an All-Rake receiver gives the following decision variable:

$$\begin{aligned} z_k^{AR} &= \frac{(\mathbf{C}_k \boldsymbol{x}_k)^T}{\|\mathbf{C}_k \boldsymbol{x}_k\|} \mathbf{y} = \sum_{j=1}^{K} \frac{(\mathbf{C}_k \boldsymbol{x}_k)^T}{\|\mathbf{C}_k \boldsymbol{x}_k\|} \mathbf{C}_j \boldsymbol{x}_j b_j + \frac{(\mathbf{C}_k \boldsymbol{x}_k)^T}{\|\mathbf{C}_k \boldsymbol{x}_k\|} \boldsymbol{n} \\ &= \|\mathbf{C}_k \boldsymbol{x}_k\| \, b_k + S_k + I_k + \nu_k \end{aligned} \tag{3.1.11}$$

where the k-th pair is the reference one. S_k and I_k represents the *interframe interference* and the *multiuser interference*, and $\nu_k \sim \mathcal{N}(0, {}^{N_0}/_2)$ is filtered thermal noise.

With Time Reversal, the decision variable for user k becomes:

$$z_k^{TR} = \sum_{j=1}^{K} \boldsymbol{e}_k^T \mathbf{C}_k \mathbf{P}_k \boldsymbol{x}_k b_k + \boldsymbol{e}_k^T \boldsymbol{n} \tag{3.1.12}$$

where $\boldsymbol{e}_k$ is the canonical vector for user k, constructed following the same rules of equation (3.1.8).

In multiuser scenarios, the equivalence between the two structures does not hold.

3.2 PERFORMANCE EVALUATION

In the proposed model, two performance measures are considered.

In the *uncoded* regime, the BER - *i.e.* bit error ratio - is taken into account.

In the *coded* regime, *mutual information* with Gaussian inputs, along with *spectral efficiency* and *bitrate*, is considered.

3.2.1 BER

The bit error ratio can be considered as an approximation of the *probability of error*. The estimation is more and more accurate as the observing time increase.

With reference to decision variable in (3.1.7) and (3.1.8), the prob. of error in both cases is equal to:

$$P_e = \frac{1}{2}P(z < 0|b = \sqrt{E}) + \frac{1}{2}P(z > 0|b = -\sqrt{E}) \tag{3.2.1}$$

where $E = P_u N$ is the transmitted *energy* per bit, considering that just one chip between N is selected over a frame.

3.2.2 Mutual Information

In A.1, details about mutual information and related measures can be found.

Mutual information for a generic user can be evaluated from equation (A.1.7), which is reported here:

$$I(X;Y) = H(Y) - H(Y|X) = H(Y) - H(U + Z + N|X) \tag{3.2.2}$$

where Y is the random variable after receiving stages, U is the useful signal and all the $H(\cdot)$ are differential entropies. Z contains both multiuser interference and ISI; N is thermal noise.

Mutual information can be used to obtain lower bounds on *capacity*. In simulations, Gaussian inputs are used: in this case, the first term of equation (3.2.2) is maximized.

As for the second term, knowing the channel and thus U, and being $H(\cdot)$ invariant to translations, it is possible to write:

$$H(U + Z + N|X) = H(Z + N) \tag{3.2.3}$$

which leads to:

$$I(X;Y) = H(Y) - H(Z + N) \tag{3.2.4}$$

In simulations, mutual information is evaluated with equation (3.2.4). All the entropies are evaluated with numerical integration methods.

From mutual information, *spectral efficiency* is derived as follows:

$$\mathcal{R} = \frac{K}{N}I(X;Y) \tag{3.2.5}$$

measured in (b/s)/Hz.

The sum-bitrate in (b/s) is obtained after bandwidth normalization:

$$R = W\frac{K}{N}I(X;Y) \tag{3.2.6}$$

3.3 TIME REVERSAL IMPLEMENTATION

Rather than just evaluate the differences between scenarios where precoding is used or not, it is interesting to exploit the various possibilities that Time Reversal offers.

How is it possible to alter its classical behavior? Two options are considered, even though there exist more.

Time Reversal towards the Generic Receiver

Under this section, the standard, classical Time Reversal is described.

The precoding impulse response for the generic user k is evaluated from its own channel impulse response.

In a decentralize ad-hoc network, the different channel conditions to which the users signals are subjected to, translate into *non-peaked* precoded impulse responses. In fact, if the generic pair k has an impulse response h_k and the impulse response between the reference receiver and the transmitter of the pair k is denoted with h_r, the overall impulse response to which the signals of transmitter k are subjected to is as follows:

$$h_k(-t) * h_r(t) \tag{3.3.1}$$

The two impulse responses exhibit a decreased correlation, leading to the *non-peaked* behavior mentioned before.

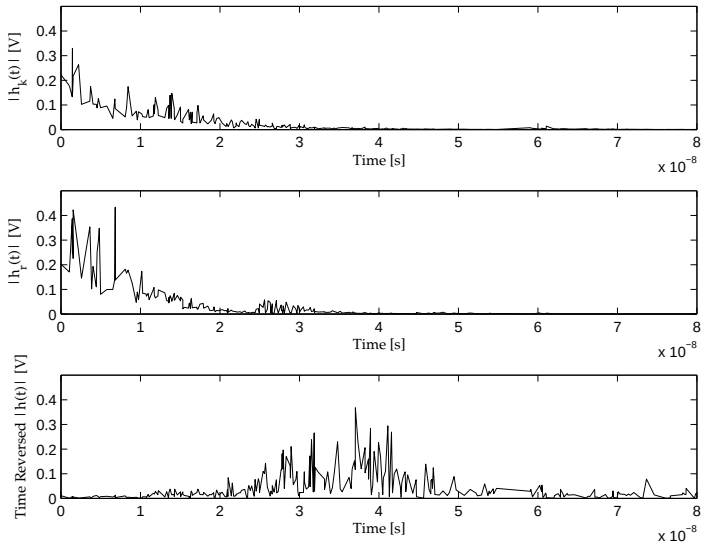

Figure 3.3-3: Impulse response after pre-filtering with $h_k(t) \neq h_r(t)$.

Figure 3.3-3 shows the overall impulse response in this case. The peak is not visible and the impulse response spreads over time axis, due to the decreased correlation.

Time Reversal towards the Reference Receiver

In an ad-hoc network, it could be interesting to privilege one pair among K.

Here, the precoding impulse response for the generic user k depends on the impulse response that is found between its transmitter and the reference receiver.

This makes the interference from user k at the reference receiver more impulsive.

In this case, the reference pair could be favoured.

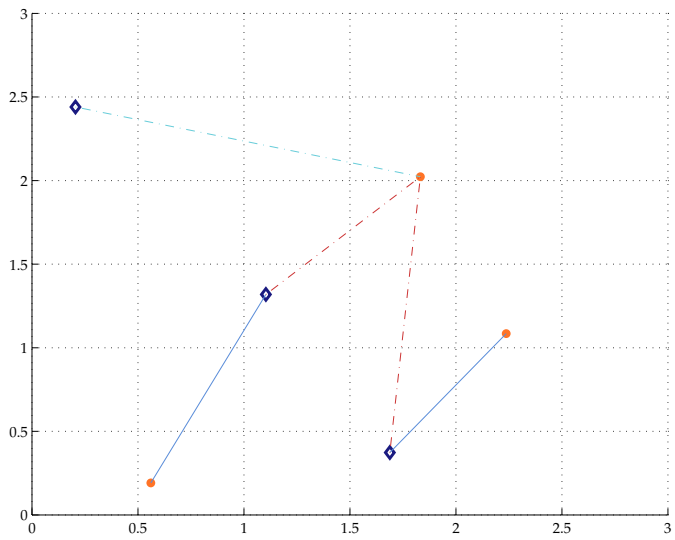

Figure 3.3-4: Links found in a network scenario where $K = 3$ pairs communicate. As usual, the reference link is the paler blue one.

Figure 3.3-4 highlights all the links between transmitters and receivers which can be found in a network scenario where $K = 3$ pairs communicate.

Each link has its own associated channel impulse response: along with red links, impulse responses h_r are used. In case of blue links, signals from transmitter k are subjected to its own pair's impulse response h_k.

3.4 THE IEEE 802.15.3A UWB CHANNEL MODEL

The large bandwidth of UWB channels gives rise to new effects compared to conventional wireless channels: multipath-rich profile and non-*Rayleigh* fading are the main distinguishing characteristics.

There is an extensive literature on UWB channel modeling. The most comprehensive effort was undertaken by the Channel-Modeling committee of the IEEE 802.15.3a group.

Three components were considered for developing the proposed model: Large-Scale Fading, Small-Scale Fading and the S-V Model.

In fact, the signals received in radio environments are exposed to rapid fluctuations (Small-Scale Fading), which arise when the user moves for distances in the order of several dozen wavelengths, and to slow fluctuations (Large-Scale Fading), due to path loss in relation to distance. Slow fading - which in UWB is *hardly* ever *frequency independent* - can be also correlated to *shadowing* events.

3.4.1 Large-Scale Fading

The path loss is based on free space model given as:

$$L = 20\log(4\pi f_c d/c) \tag{3.4.1}$$

where $f_c = \sqrt{f_L f_H}$ and f_L and f_H are -10 dB lower and upper frequencies.

The shadowing effect is found to be *lognormally* distributed with a standard deviation of 3 dB: its distribution controls the mean value of the distribution of the rapid fluctuations.

3.4.2 Small-Scale Fading

As for small-scale fading, the Channel-Modeling committee examined three channel models: TD Line, Δ-K and Saleh-Valenzuela (S-V) model. The latter, modified with lognormal multipath amplitude, was found to best fit indoor-made UWB measurement campaigns.

S-V Model

The S-V model is based on the observation that multipath contributions related to the same pulse arrive at the receiver grouped into *clusters*[1].

In the S-V model, the time of arrival of clusters is modeled as a Poisson arrival process with rate Λ:

$$p(T_n|T_{n-1}) = \Lambda e^{-\Lambda(T_n - T_{n-1})} \tag{3.4.2}$$

where T_n and T_{n-1} are the times of arrival of the n-th and the $(n-1)$-th clusters.

Within each cluster, subsequent multipath contributions also arrive according to a Poisson process, but with rate λ:

$$p(\tau_{nk}|\tau_{(n-1)k}) = \lambda e^{-\lambda(\tau_{nk} - \tau_{(n-1)k})} \tag{3.4.3}$$

where τ_{nk} and $\tau_{(n-1)k}$ are the times of arrival of the n-th and the $(n-1)$-th contributions within cluster k.

The gain of the n-th replica in the k-th cluster is a real random variable a_n with modulus β_{nk} and phase θ_{nk}. As said before, the values of β_{nk} are assumed to be indipendent and *lognormally* distributed. Instead, the values of θ_{nk} are assumed to be indipendent and *uniformly* distributed over $[-\pi, +\pi]$.

The IEEE 802.15.3a channel impulse response can be expressed as:

$$h(t) = X \sum_{n=1}^{N} \sum_{k=1}^{K_n} \alpha_{nk} \delta(t - T_n - \tau_{nk}) \tag{3.4.4}$$

where X is a lognormal random variable representing the amplitude gain of the channel, N is the number of observed clusters, K_n is the number of multipath contributions received within the n-th cluster and α_{nk} is the channel coefficient of the k-th multipath replica of the n-th cluster, which can be defined as:

$$\alpha_{nk} = p_{nk}\beta_{nk} \tag{3.4.5}$$

where p_{nk} is a discrete random variable assuming values ± 1, accounting for signal inversion due to reflections.

1 Since UWB waveforms can be up to 7.5 GHz wide, different parts of the same object give rise to several multipath components.

The term β_{nk} can be expressed as:

$$\beta_{nk} = 10^{(x_{nk}/20)} \tag{3.4.6}$$

where x_{nk} is assumed to be a Gaussian random variable with mean μ_{nk} and standard deviation σ_{nk}. This random variable can be further decomposed as follows:

$$x_{nk} = \mu_{nk} + \xi_{nk} + \zeta_{nk} \tag{3.4.7}$$

where ξ_{nk} and ζ_{nk} are Gaussian random variables which represent the fluctuations of the channel coefficient on each cluster and on each contributions.

The value of μ_{nk} is determined to reproduce the exponential power decline for the amplitude of clusters and their relative contributions.

The amplitude gain X is expressed as:

$$X = 10^{(g/20)} \tag{3.4.8}$$

where g is a Gaussian random variable with mean g_0 and variance σ_g^2.

Table 4: Parameter settings for the IEEE 802.15.3a UWB channel model.

Scenario	Λ (1/ns)	λ (1/ns)	Γ	γ	σ_ξ	σ_ζ (dB)	σ_g (dB)
LOS (0-4m)	0.0233	2.5	7.1	4.3	3.3941	3.3941	3
NLOS (0-4m)	0.4	0.5	5.5	6.7	3.3941	3.3941	3
NLOS (4-10m)	0.0667	2.1	14	7.9	3.3941	3.3941	3
Extreme NLOS	0.0667	2.1	24	12	3.3941	3.3941	3

According to the above definitions, the channel model in equation (3.4.4) is *completely* described after the following parameters:

- The cluster average arrival rate Λ (1/ns)
- The replica average arrival rate λ (1/ns)
- The power decay factor Γ for clusters (dB/ns)
- The power decay factor γ for replicas within a cluster (dB/ns)
- The standard deviation σ_ξ of the fluctuations of the channel coefficients for clusters (dB)
- The standard deviation σ_ζ of the fluctuations of the channel coefficients for replicas (dB)

- The standard deviation σ_g of the channel amplitude gain (dB)

In the IEEE 802.15.3a standard, an initial set of values for the above parameters is suggested. These values were tuned to fit the measurements data of several scenarios, which are shown in Table 4.

This model defines a continuos time multipath channel model: an example of realization can be found in Figure 2.3-6. Its nature allows to evaluate an equivalent discrete/sampled time channel after a time scan of the multipath contributions, with an appropriate step size.

4 ANALYSIS OF SIMULATION RESULTS

Contents

This chapter presents the results obtained after the simulations. There are various parameters which are common to each one simulation: users channels are derived from the IEEE 802.15.3a model, LOS (0-4m), which is suitable for the presumed applications of an ad-hoc UWB network. In particular, the *delay spread* of each channel is fixed at 50 ns, which includes the most essential replicas, Ferrante et al., 2013. Each channel is considered to be *stationary* in the observation time.

All simulations are done assuming perfect channel knowledge, *i.e.* perfect CSI, except where otherwise specified.

In each iteration, 5000 or more frames are considered, divided in N chips whose length is 1 ns. The transmitted waveform is adapted to the chip length. Channels and users positions, thus network arrangement, are modified throughout the Monte Carlo experiments.

In order to consider *asynchronism* between users, each interfering signal is shifted in time. Perfect timing is instead assumed between each receiver and its intended transmitter.

Concerning thermal noise, it has a fixed variance $\sigma_n^2 = 1$. Useful signals power varies with SNR.

4.1 SINGLE USER CHANNEL

While the multiuser case is useful to emphasize how multiuser interference affects the overall transmission, the single user case allows to evaluate the receivers in relation to thermal noise and ISI/IFI.

4.1.1 Interframe Interference

As said in section 3.1.2, the single user scenario highlights the presence of the interframe interference.

The following simulations are carried out in a fictional scenario where no thermal noise is added to the received signal. In this case, the performance is *exclusively* related to the interframe interference.

In such conditions, a real PDF of interframe interference can be evaluated: in Figure 4.1-1, PDFs are shown in relation to frame length and receiver kind, along with Gaussian PDFs with same variance and mean value.

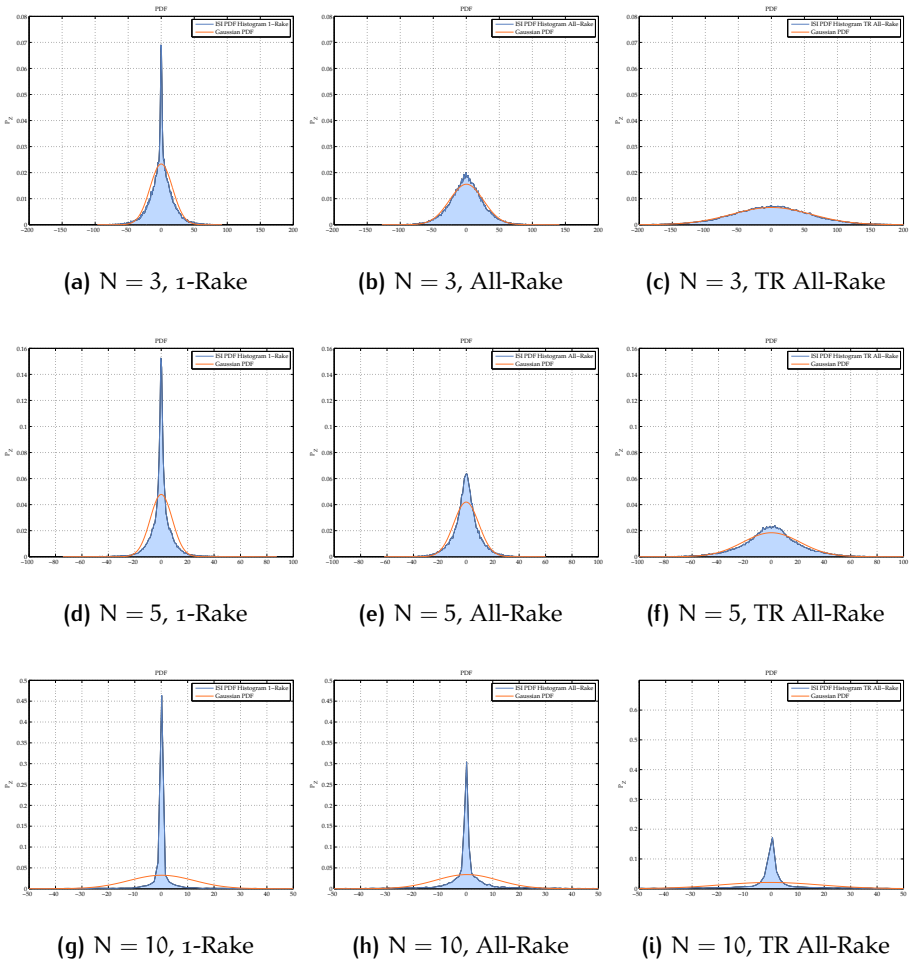

(a) N = 3, 1-Rake **(b)** N = 3, All-Rake **(c)** N = 3, TR All-Rake

(d) N = 5, 1-Rake **(e)** N = 5, All-Rake **(f)** N = 5, TR All-Rake

(g) N = 10, 1-Rake **(h)** N = 10, All-Rake **(i)** N = 10, TR All-Rake

Figure 4.1-1: Interframe interference PDF with several receivers and frame lengths: the UWB channel is truncated to 50 ns.

In Figure 4.1-1, it is possible to observe two important behaviors of the interframe interference.

First and foremost, the reasonable reaching of more impulsive PDFs, due to the increase of the frame length N: this behavior is irrespective of the receiver used.

It is not hard to find in literature the assumption of high enough frame lengths to avoid interframe interference: that works, although with a high price in terms of bitrate. It could also be possible to select less paths in the impulse response, with a concrete reduction in performance.

On the other hand, it is important to notice the better robustness to interframe interference in 1-Rake receivers, which outperform all the others. Indeed, interframe interference cause a significant degradation in TR-UWB communications above all, where a larger transmitted waveform - close to doubling the length of the received signal - is adopted. Moreover, Time Reversal increases signal power, making IFI/ISI more strong. This phenomenon is highlighted in TR All-Rake schemes.

All-Rake and TR 1-Rake receivers behave in the same manner; in these figures, just the All-Rake receiver is shown.

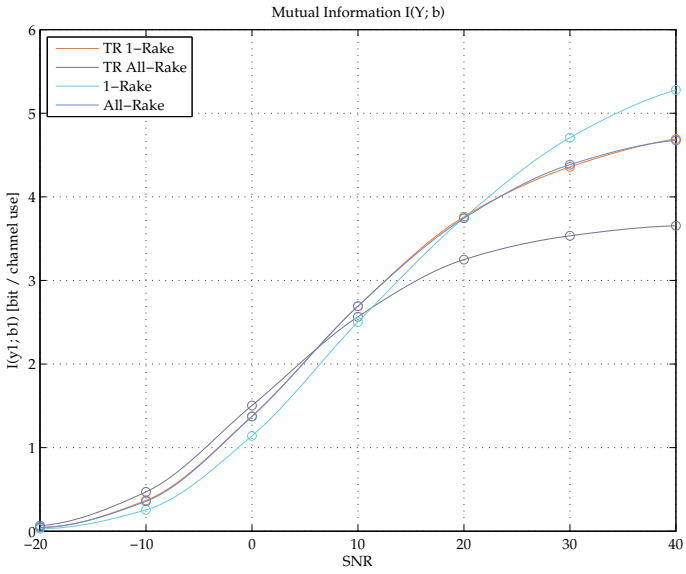

Figure 4.1-2: Mutual information vs SNR in a single user scenario with IFI/ISI and N = 10.

Figures 4.1-2 and 4.1-3 show how the behavior found in PDFs is reflected into mutual information. Here thermal noise is added.

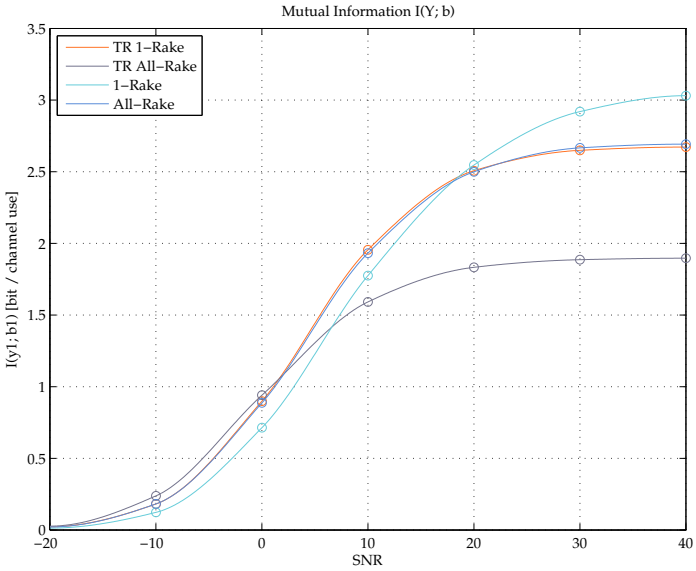

Figure 4.1-3: Mutual information vs SNR in a single user scenario with IFI/ISI and $N = 5$.

In noise limited scenarios, where ISI/IFI is negligible, it is possible to observe the theoretical trend.

TR All-Rake outperforms all the other receivers, while the All-Rake and the TR 1-Rake have same performance.

Whereas in ISI/IFI limited scenarios, it is observable a reversal of the trend, with 1-Rake outperforming all the others receivers. The TR All-Rake *rapidly* reaches a lower mutual information floor as the transmitted power increase.

To mitigate this phenomenon, various filters can be implemented. In the next subsection, a simple non-linear equalizer is described.

Decision Feedback Equalizer

Adaptive equalization is a well known technique to suppress ISI. In UWB communications, the Rake receiver should be combined with an equalizer capable to estimate and equalize the UWB channel. In literature, Zero-Forcing, MMSE and other linear equalizers have been evaluated in UWB contexts. An example can be found in Eslami and Dong, 2005.

However, UWB channels are channel with severe ISI and deep spectral nulls in their impulse responses: in this case, non-linear equalizers are an obvious choice.

A *decision feedback equalizer* makes use of previous decisions in attempting to estimate the current bit with a *symbol-by-symbol* detector.

A DFE estimates the channel impulse response and *not* its inverse, as linear equalizer do. So, it does not suffer from noise enhancement.

The interframe interference that comes from previous frames is reconstructed and then subtracted.

There are different variations of decision feedback equalizers. In general, a DFE consists of one *feed-forward* filter, one *feed-back* causal filter and a simple detector. In UWB communications, the feed-forward filter is a Rake receiver.

An example scheme is in Figure 4.1-4.

Since an assumption of perfect channel estimation is made in this work, no estimation technique is explained in detail: in digital communications, LMS-based techniques can be useful, as shown in Chung et al., 2007.

However, degradation in DFEs performance occurs when incorrect bits are fed through the feedback loop. Then instead of mitigating ISI, the equalizer enhances ISI. Moreover, error propagation could cause *burst* of decision errors and a corresponding increase in BER.

Various techniques for mitigating error propagation have been proposed. Chiani, 1997 evaluated a solution based on the introduction of erasures, related to a threshold T.

The idea is simple: if the sample at the input of the decisor is close to the threshold, the corresponding output is considered unreliable.

The erasure criterion can be stated as follows:

$$\begin{cases} Z \geqslant T & \text{feedback } 1 \\ |Z| < T & \text{unreliable: feedback } 0 \\ Z \leqslant -T & \text{feedback -1} \end{cases} \tag{4.1.1}$$

where Z is the input at the decisor and T can be varied according to the signal power.

This is the solution which is implemented in simulations, in uncoded regime.

In Figure 4.1-5, the complete suppression of interframe interference obtained with the introduction of a guard time before each frame, leads to the expected and well-known theoretical behavior.

With more than 8 bits per channel use - *i.e.* NT_c - UWB communications can *potentially* reach impressive transmission bitrates.

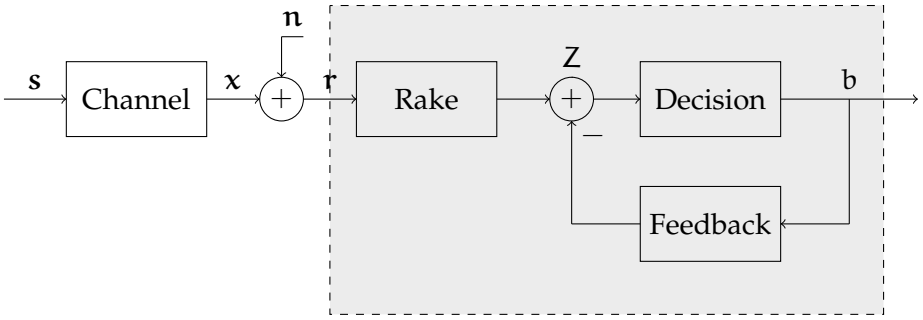

Figure 4.1-4: Decision feedback equalizer block diagram in UWB communications. The Feedback output could also be subtracted *before* the Rake receiver.

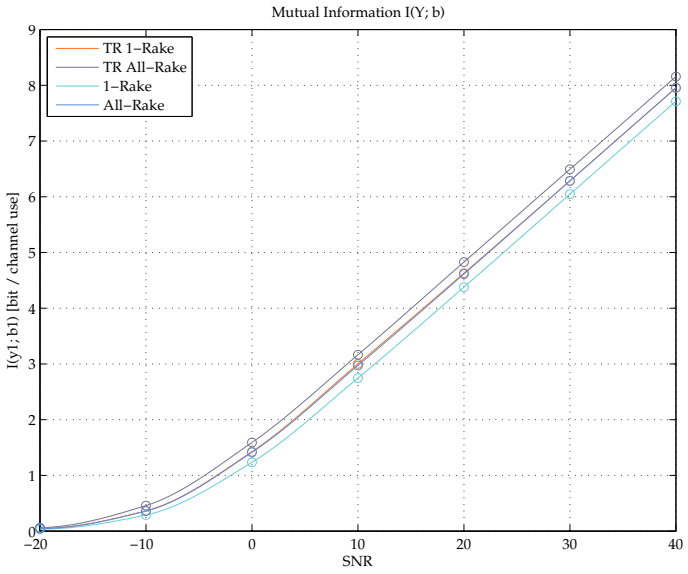

Figure 4.1-5: Mutual information in a single user scenario with N = 10 after ISI removal.

4.2 MULTIUSER CHANNEL

In the multiuser case, multiuser interference becomes the most important interference term. The following results are obtained after ISI cancellation[1], except where otherwise specified, in order to highlight how multiuser interference behaves under different network conditions. Since each receiver works with its associated transmitter, ISI is cancelled just for the reference pair[2].

1 Through DFE in uncoded regime, and through time guards in coded one.

2 The reference receiver does not know other users channel properties, thus multiuser interference comes together with ISI of each other pair.

4.2.1 Multiuser Interference

In this section, PDFs characteristics when SNR = 20 dB and performance related to multiuser interference are presented.

Simulations shows that multiuser interference is in general *not* Gaussian, irrespective of precoding and receiver stages, confirming other studies. This is due to the impulsive nature of TH-UWB signals.

In TH-UWB communications, the frame duration is much longer than the pulse duration, and here, just a single pulse is transmitted per frame. Therefore, in a given chip, strong interference comes from few users compared to the number of total interfering users. Also, the propagation characteristics of UWB signals suggest a small number of interfering users at close range. This is in contrast to usual CDMA communications which have a wide coverage area and contributing interferers of lower relative power.

These properties lead to an interference PDF which is not Gaussian. In fact, the peak and the tail of the histograms cannot be modeled with a Gaussian distribution, with the exception of some particular cases.

This result has a powerful impact over the entire performance of the network: since Gaussian random variables maximize $H(\cdot)$, it is desirable to achieve impulsive interference PDFs, in order to make the second term in equation (3.2.4) smaller.

As expected, multiuser interference creates a mutual information floor, which is lower as the number of users in the network increase.

Some cases are evaluated in the following lines, while Time Reversal - with classical, standard implementation as described in 3.3 - is compared to non-precoded transmissions.

Performance under low loads, low number of users

In this case, multiuser interference is rather little and performance *strongly* depends on the position of the users and on the amount of misalignment in time between them. Thus, it is hard to determine an overall, common behavior.

This case is however useful to evaluate how some parameters, such as distance, influence multiuser interference.

First of all, PDFs reports *non-gaussianity* of multiuser interference.

Figure 4.2-6 reports multiuser interference PDFs for several cases, along with a reference Gaussian with same variance and mean value.

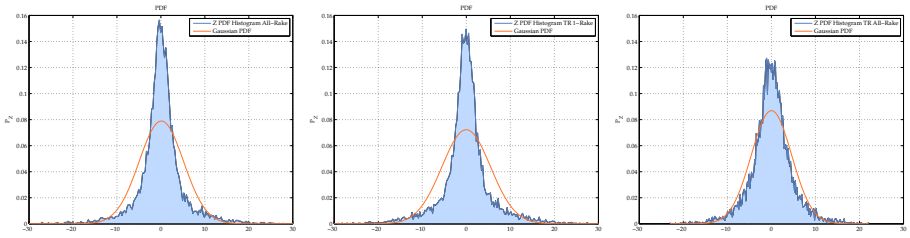

(a) All-Rake, k = 8.901 **(b)** TR 1-Rake, k = 7.683 **(c)** TR All-Rake, k = 5.310

Figure 4.2-6: Multiuser interference PDF and associated *kurtosis* with K = 2, N = 8 and Load = 0.25. Near users (≈ 1m).

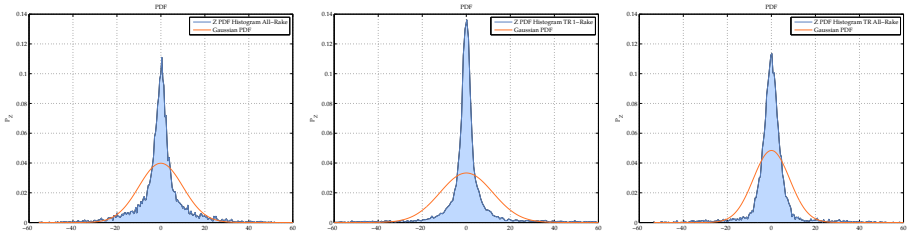

(a) All-Rake, k = 9.809 **(b)** TR 1-Rake, k = 17.886 **(c)** TR All-Rake, k = 12.24

Figure 4.2-7: Multiuser interference PDF and associated *kurtosis* with K = 2, N = 8 and Load = 0.25. Far users (≈ 8m).

Time Reversal does not help in reaching more impulsive PDFs: the classical All-Rake shows higher kurtosis, which is a common parameter used to measure Gaussian-likeness, for which k = 3.

This is due to different factors: first of all, impulse responses do not have a real peak when Time Reversal is implemented as in the first part of section 3.3. This reduces TR capabilities towards signals impulsiveness.

In addition, the power and length increase to which time reversed signals are subjected to does not help. Without power control, the presence of strong interference near the reference receiver is catastrophic. Time Reversal increase even more this phenomenon.

In fact, in Figure 4.2-6, users are near, with maximum distance 1 m.

Distance can improve Time Reversal performance, as Figure 4.2-7 reports. This behavior suggests to use *power control* in order to improve Time Reversal capabilities.

Performance under low loads, high number of users

Under this scenario, the frame length is comparable to the number of users - *i.e.* N ~ K. In the next cases, an average maximum distance (≈ 4m) is chosen to evaluate performance.

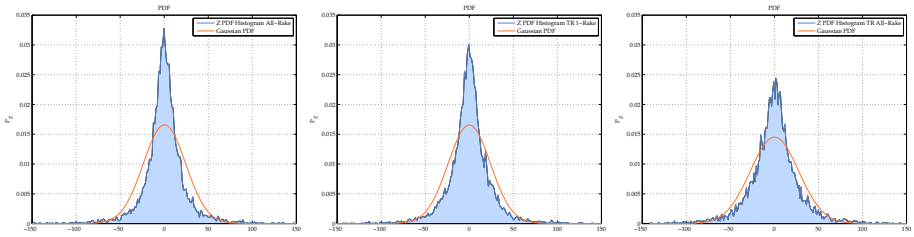

(a) All-Rake, k = 6.797 **(b)** TR 1-Rake, k = 6.448 **(c)** TR All-Rake, k = 5.943

Figure 4.2-8: Multiuser interference PDF and associated *kurtosis* with K = 10, N = 20 and Load = 0.5.

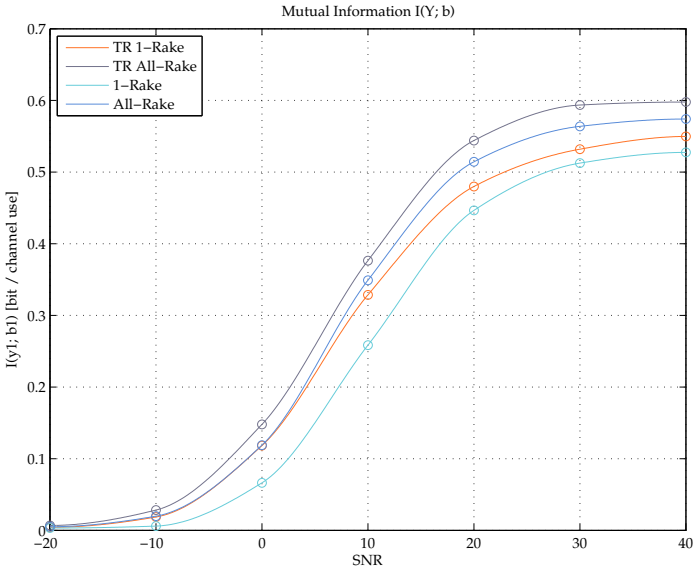

Figure 4.2-9: Mutual information vs SNR with K = 10, N = 20 and Load = 0.5.

Figure 4.2-9 shows that Time Reversal does not perform well. In fact, the All-Rake receiver outperforms its precoded equivalent. So the *near-far* problem is still an issue.

TR All-Rake exhibits the best performance; however, it has much higher *complexity* than the other receivers.

Performance under high loads, high number of users

When the network is *heavily* loaded, and N is little compared to K, multiuser interference approaches Gaussian distributions.

In this case, Time Reversal is performing well, achieving higher kurtosis than non-precoded equivalents. Both in the 1-Rake and in the All-Rake cases, precoded transmissions experience higher performance. This is due to the PDF altering properties of time reversed communications, which are *particularly* observable in scenarios with rich and varied multiuser interference, in which the problems described before for precoded transmissions are attenuated, due to the high number of users.

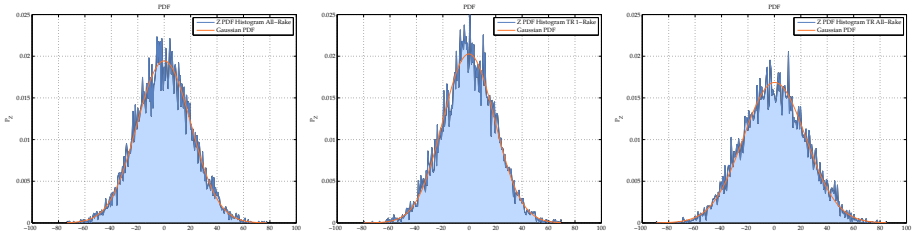

(a) All-Rake, k = 3.106 **(b)** TR 1-Rake, k = 3.219 **(c)** TR All-Rake, k = 3.177

Figure 4.2-10: Multiuser interference PDF and associated *kurtosis* with K = 20, N = 5 and Load = 4.

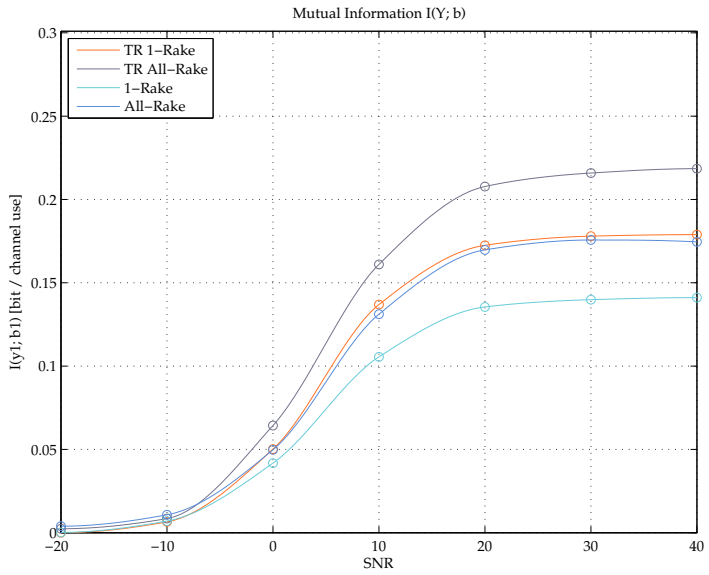

Figure 4.2-11: Mutual information vs SNR with K = 20, N = 5 and Load = 4.

4.2.2 Power Control and TR Implementations

As seen, strong interference near the reference receiver is a big issue when Time Reversal is adopted.

Power control, *i.e.* a technique for which each signal is adapted to arrive at the reference receiver with an equal power, can be used.

In a network where no coordinated operations are possible, power control can be rather hard to implement. Nonetheless, it is important to exploit how performance is affected.

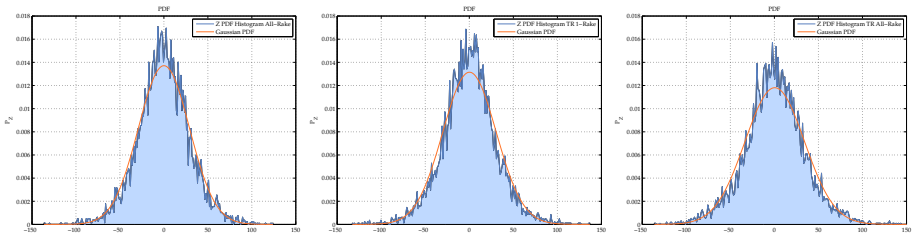

(a) All-Rake, k = 3.427 **(b)** TR 1-Rake, k = 3.772 **(c)** TR All-Rake, k = 3.593

Figure 4.2-12: Multiuser interference PDF and associated *kurtosis* with K = 10, N = 20 and Load = 0.5 in *perfect* power control.

Comparing Figure 4.2-12 to Figure 4.2-8, which account for the same scenario, it can be seen that power control makes time reversed multiuser interference more impulsive than non-reversed one, even without changing time reversal implementation to the second one described in section 3.3 - *i.e.* the peaked version.

However, power control makes PDFs more Gaussian: the lack of power control needs a higher number of users in order to fit the Gaussian approximation[3].

Figure 4.2-13 shows how power control is able to increase performance of precoded transmission. While the 1-Rake and the All-Rake are *practically* untouched, both Time Reversal receivers are subject to a great improvement in performance, achieving higher mutual information floors.

The same happens in case of high loads and high number of users. Figure 4.2-14 reports PDFs for this case, which can be compared to those in Figure 4.2-10.

3 This is not in contrast with what stated before: impulsiveness is *always* desiderable in interference PDFs, but mutual information depends on a difference, not just from the second term in (3.2.4).

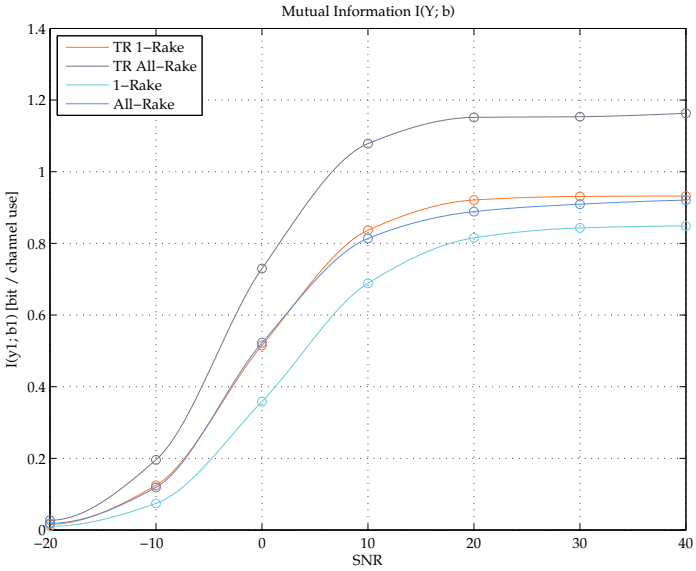

Figure 4.2-13: Mutual information vs SNR with K = 10, N = 20 and Load = 0.5 in *perfect* power control.

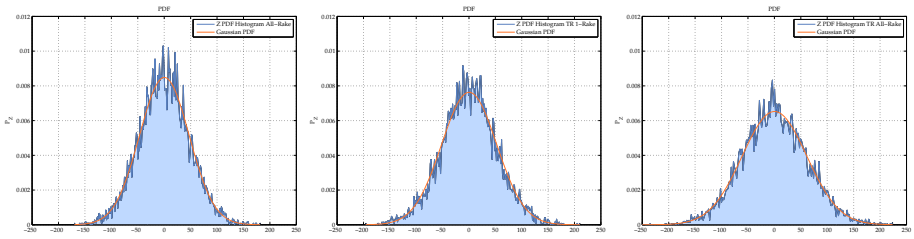

(a) All-Rake, k = 3.022 **(b)** TR 1-Rake, k = 3.189 **(c)** TR All-Rake, k = 3.137

Figure 4.2-14: Multiuser interference PDF and associated *kurtosis* with K = 20, N = 5 and Load = 4 in *perfect* power control.

Time Reversal towards the Reference Receiver

When TR is based on the channel between the generic transmitter and the reference receiver, the overall impulse response to which interfering signals are subjected to has a peak.

It is important to note that is indeed quite unpractical to implement Time Reversal in this manner. In particular, it is impossible in a network when pairs do not communicate between each other[4].

4 In the particular case in which the reference pair transmits its channel state informations to all other pairs, it could be possible to establish this kind of Time Reversal. In a scenario like this, the reference pair should *partially* act as a *base station*. An increase in both *complexity* and *overload* should be considered.

In Figure 4.2-15, performance in terms of BER is depicted. As it can be seen, Time Reversal based on the channel between the generic transmitter and the reference receiver (TR Mod1) does not show performance increase.

The same behavior is also found in relation to mutual information, as Figure 4.2-17 reports.

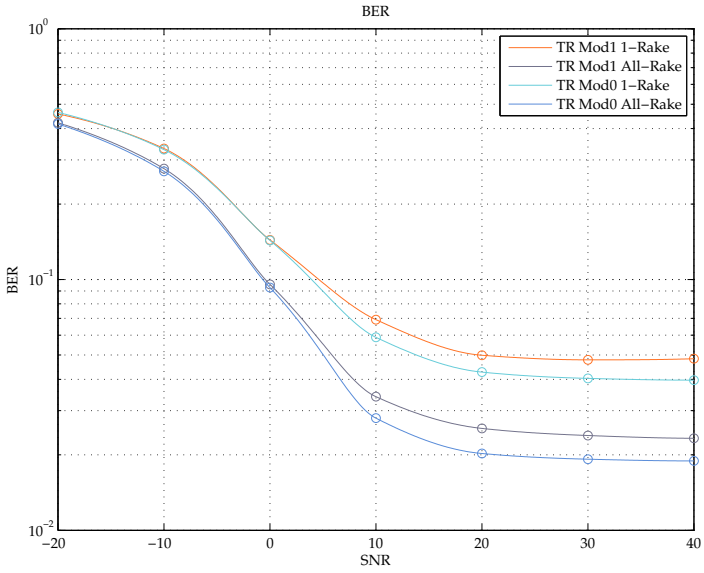

Figure 4.2-15: BER vs SNR with K = 10, N = 20 and Load = 0.5. Comparison between two Time Reversal schemes.

In fact, although in this case greater impulsiveness is reached, it is to consider that interfering signals bear more power and are emphasised due to the peak in the overall channel impulse response, which is *anyway* selected with a high prob. at the reference receiver.

Moreover, ISI/IFI enhances this phenomenon: more peaks are found in overlapping frames.

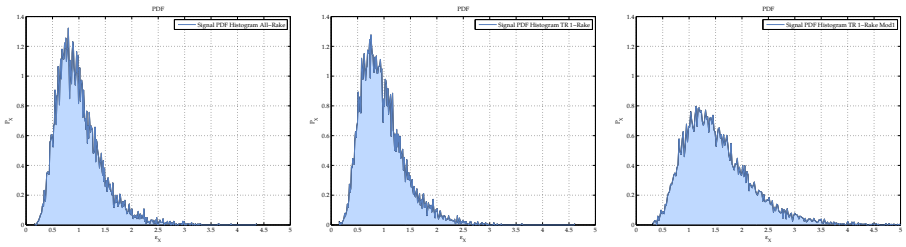

(a) All-Rake **(b)** TR 1-Rake Mod0 **(c)** TR 1-Rake Mod1

Figure 4.2-16: Normalized *energy* of interfering signal in different cases.

Figure 4.2-16 highlights the power increase in TR Mod1 schemes: it is the worst case. Instead, when TR Mod0 is used, interfering power is quasi-identical and comparable to that of non-precoded transmissions.

So it is possible to conclude that Time Reversal performance towards multiuser interference *strongly* depends on the corrrelation between the impulse responses which form the overall impulse response. In this case, the fact that it is difficult to adopt this TR scheme turns out to be a good thing.

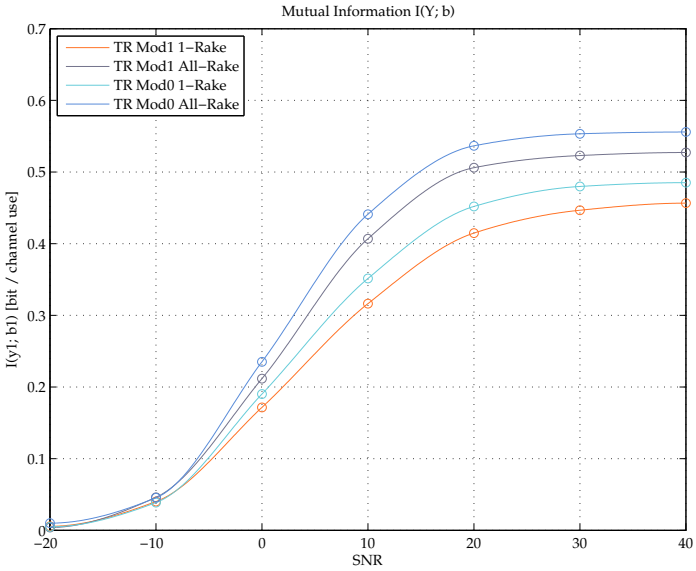

Figure 4.2-17: Mutual information vs SNR with K = 10, N = 20 and Load = 0.5. Comparison between two Time Reversal schemes.

4.2.3 Robustness to Channel Estimation Errors

When the channel is not *perfectly* estimated, Rake receivers are subject to a loss in performance. The loss comes both from a correlation decrease between receivers masks and received signals and a non-perfect ISI/IFI cancellation.

As seen in the previous section 4.1, Time Reversal is less robust to ISI in respect to non-precoded transmissions. This is *mostly* due to the increased length and power of precoded signals.

In case of channel estimation errors, it is to expect a great loss in Time Reversal performance.

In simulations, estimation errors are modeled and added as Gaussian noise to the impulse responses. In particular, the convolution matrices C and P are evaluated on:

$$\widehat{h}(t) = \sqrt{1-\tau^2}h(t) + \tau\xi(t) \tag{4.2.1}$$

where ξ is white Gaussian noise with standard deviation $0 < \tau < 1$. When $\tau = 0$, the impulse responses are *perfectly* estimated; when $\tau = 1$, the estimated impulse responses are *independent* from the real $h(t)$.

Figure 4.2-18 and Figure 4.2-19 compare the same scenario with different τ.

Since no perfect channel is known, results are evaluated just in terms of BER. In this case, mutual information cannot be evaluated following (3.2.4), which requires perfect channel knowledge.

As it can be seen, Time Reversal receivers are the ones which experience the greatest performance loss. Indeed, TR 1-Rake turns to be worse even than the simplest 1-Rake, whose performance is just related to the reappearance of ISI/IFI. In fact, there is no need to estimate channels in a 1-Rake scheme.

On the other hand, TR All-Rake, which need a double channel estimation - one in transmission and the other in reception - is the most degraded scheme.

Table 5: Percentage increase of BER floor with $\tau = 0.1$.

Receiver	Percentage
TR 1-Rake	58%
TR All-Rake	65%
1-Rake	7%
All-Rake	15%

Table 5 shows percentage increase of the BER floor for each scheme. As said, precoded transmissions are the most degraded ones, while the 1-Rake exhibits a little worsening *only* due to the reappearance of ISI/IFI.

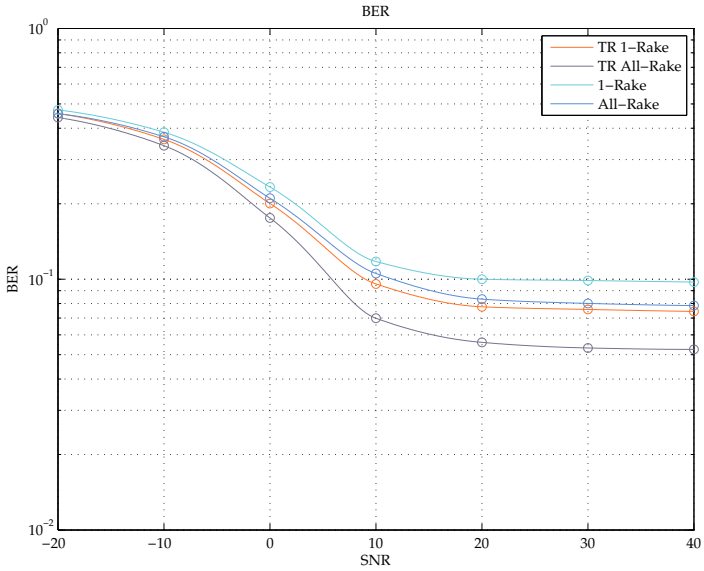

Figure 4.2-18: BER vs SNR with K = 10, N = 20 and Load = 0.5. $\tau = 0$.

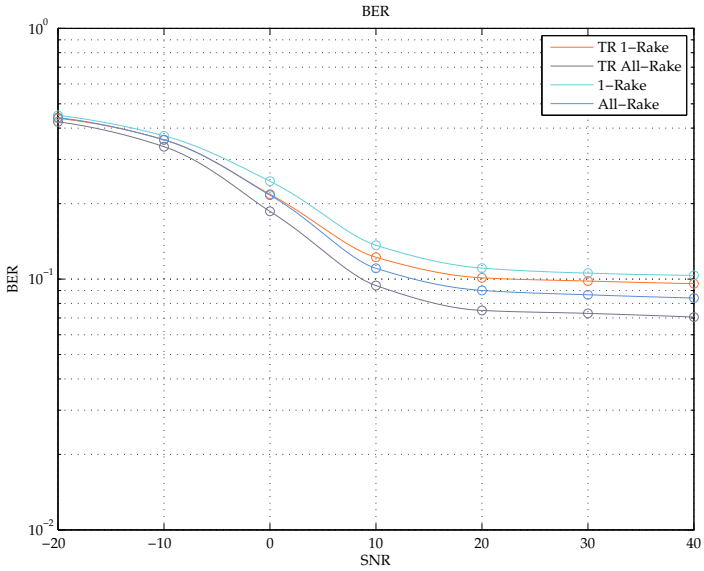

Figure 4.2-19: BER vs SNR with K = 10, N = 20 and Load = 0.5. $\tau = 0.01$.

5 CONCLUSIONS

This work highlighted differences between Time Reversal precoded transmissions and non-precoded ones, along with Rake receivers, in an ad-hoc *uncoordinated* network.

In order to evaluate these techniques, a discrete or sampled-time model was adopted: results were divided in single and multiuser cases.

In the single user case, the importance of ISI/IFI was underlined. Time Reversal increases both length and power of signals, leading thus to small robustness towards this kind of interference. When channels impulse responses are known, IFI/ISI can be cancelled: a non-linear decision feedback equalizer was evaluated.

Concerning performance, with removed ISI/IFI, the theoretical or classical trend was experienced. TR 1-Rake and All-Rake had *identical* performance. As a consequence, Time Reversal offers the chance to achieve the same performance of an All-Rake receiver, using a simple 1-Rake, switching thus *complexity* to the transmitter side (in presence of noise but without multiuser interference).

TR All-Rake, being the most complex receiver, outperformed all the others.

In the multiuser case, results highlighted *non-gaussianity* of multiuser interference PDFs, due to the nature of impulse radio communications. In fact, a Gaussian model for multiuser interference was found to be appropriate just in *heavily* loaded contexts.

In power-unbalanced scenarios, multiuser interference PDFs also depend on the *spatial density* of interfering users. Increasing the network area, a greater impulsiveness is reached, requiring higher loads, or higher bitrates, to fit Gaussian distributions.

As known, Time Reversal can increase even more the *kurtosis* of multiuser interference PDFs, making them more impulsive, due to its time and spatial focusing properties. When received power is uncontrolled, these properties are less effective.

Indeed, simulations reported that kurtosis was higher in non-precoded transmissions as the network area was smaller. Precoded transmissions increase signal power and length, thus interference, leading to smaller robustness to the *near-far* problem. In this case, Time Reversal experienced worse performance.

When the network area was increased, precoded transmissions showed better performance, and reached higher kurtosis. This result suggested to use *power control* in order to improve TR communications.

Concerning precoded transmissions, simulations showed better performance as compared to non-precoded equivalents as the number of users were increased. In this case, properties of TR towards PDFs impulsiveness are more visible, even in no power controlled scenarios.

In order to validate results, a fictitious power control was implemented. Along with power control, precoded transmissions showed overall better performance, while non-precoded ones were *practically* untouched.

In an uncoordinated network, power control is however impossible. Under the evaluated scenarios, it seems in general reasonable to avoid precoding with Time Reversal.

Another fictitious scenario was then considered. Time Reversal was based on the channel between the generic transmitter and the reference receiver. In this case, there is maximum correlation and a *peak* in the overall impulse response to which the signals of each user are subjected to.

A decrease in performance was seen under this TR scheme. An interfering Time Reversal signal is in fact more disturbing here, since precoding increases its power. The presence of ISI/IFI enhances this phenomenon.

On the other hand, when precoding is perturbed, as *normally* happen in ad-hoc networks, TR signals bear as much power as non-precoded signals.

Uncoordinated ad-hoc networks performance under TR precoding is thus improved due to the partial, not perfect correlation that exists between the impulse responses of the users.

So, in centralized contexts - where all users communicate with the same node or base station - it is possible to have power controlled communications, but it is impossible to have TR interference without peaks; while in uncoordinated ad-hoc networks, it goes the opposite.

As a final step, robustness towards channel estimation errors was evaluated. Channel estimation errors bring ISI/IFI back in the reference user frames, while decrease signal/mask correlation at each receiver. Time Reversal communications experienced the greatest performance losses - due to worse robustness to ISI/IFI.

In particular, TR All-Rake, which need a double channel estimation, were the most degraded scheme.

So, effective channel estimation techniques, along with an appropriate control of ISI/IFI, are crucial to Time Reversal application in ad-hoc UWB networks.

Further investigations which could be made to enrich this work are: the development of more powerful ISI/IFI removal techniques. In particular, TR precoding could be improved to combat ISI/IFI in the transmitter side, without the need of a feedback block at reception; this could have a positive impact in Time Reversal communications, both in performance and *complexity*. The evaluation of more complex receivers, capable to exploit and to adapt to multiuser interference, and to endorse multi-frame processing. The consideration of coding techniques, for example a repetition code, at the expense of bitrate, to improve overall performance.

The evaluation of all these improvements should require modifications to the discrete time model presented in this work.

A APPENDIX

Contents

A.1 FUNDAMENTALS OF INFORMATION THEORY

The main result of *information theory* (IT) is the finding that error-free transmission across a non-ideal channel is possible: this happen as long as the information rate doesn't exceed the channel *capacity*.

This result is evaluable after the definition of mathematical objects able to measure information. Within Shannon's IT, the information is measured considering the statistics of *symbols* emitted by information sources.

A.1.1 Entropy

An information source emits a random discrete[1] symbol $X = x_i$ which assumes one out of M values $x_1, x_2, \ldots, x_M$ from a given *alphabet* $\mathbb{X}$. To each value, a probability of appearance is given:

$$P_X(x_i) = \Pr\{X = x_i\} \tag{A.1.1}$$

For example, a *binary* information source can emit the binary symbols $X = 0$ and $X = 1$ with probabilities $\Pr\{X = 0\} = p_0$ and $\Pr\{X = 1\} = 1 - p_0$.

1 Although the transmitted and received signals are continuous-valued in the physical channels, the communication problem is discrete in nature: the transmitter sends one codeword and the receiver would like to figure out which codeword is transmitted out of a finite number of them.

The average information associated with the symbol X is given by the *entropy*, measured in bit:

$$H(X) = -\sum_{i=1}^{M} p_X(x_i) \log_2(p_X(x_i)) \tag{A.1.2}$$

To better understand this definition, consider an information source emitting letters from the italian *alphabet*.

In order to figure out a word, the first letters are important: in the italian language just few words starts with the letter h, that is, the letter h bears more information than the letter m when it comes to distinguish several words.

Shannon demonstrated that the *only* function which could *perfectly* represent the information associated to an event, *i.e.* a *symbol*, was $-\log_2(p_X(x_i))$. This function translates in maths the fact for which a surprising *symbol* bears more information than an expected one. Averaging on each *symbol*, returns the equation (A.1.2).

The entropy can thus be interpreted as a measure of the amount of *uncertainty* associated with the random variable x. From equation (A.1.2) it comes that $H(X)$ is *always* non-negative and equal to zero if X is deterministic.

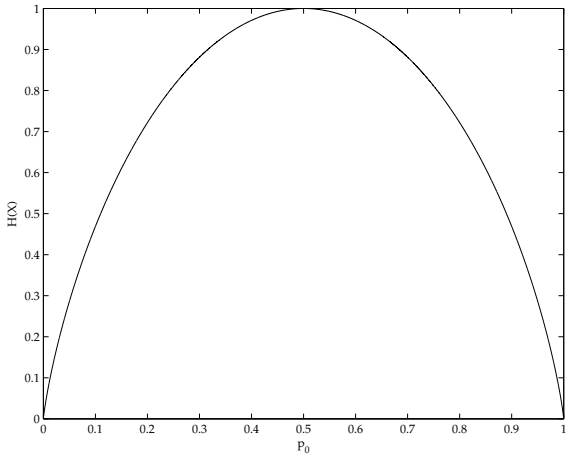

Figure A.1-1: Entropy of a binary-valued random variable x which takes on the values with probabilities p_0 and $1 - p_0$.

The definition of entropy can be extended by considering two random variables. Here, X refers to the input symbol and Y denotes the output symbol or received symbol, thus originating a channel model.

With M input symbol values and N output symbol values, the *joint entropy* is defined as follows:

$$H(X,Y) = -\sum_{i=1}^{M}\sum_{j=1}^{N} p_{X,Y}(X,Y)\log_2(p_{X,Y}(X,Y)) \tag{A.1.3}$$

The entropy of X conditional on $Y = j$ is quickly defined to be:

$$H(X|Y=j) = -\sum_{i=1}^{M} p_{X|Y}(x_i|y_j)\log_2(p_{X|Y}(x_i|y_j)) \tag{A.1.4}$$

This can be interpreted as the amount of uncertainty left in X after observing that $Y = j$. The conditional entropy of X given Y is the mean value of equation (A.1.4), averaged over all possible values of Y:

$$\begin{aligned} H(X|Y) &= -\sum_{j=1}^{N} p_Y(y_j)H(X|Y=j)) = \\ &= -\sum_{i=1}^{M}\sum_{j=1}^{N} p_{X,Y}(x_i,y_j)\log_2(p_{X|Y}(x_i|y_j)) \end{aligned} \tag{A.1.5}$$

One would expect that conditioning reduces uncertainty, and in fact it can be shown that:

$$H(X|Y) \leqslant H(X) \tag{A.1.6}$$

It becomes an equality when X and Y are indipendent random variables.

A.1.2 Mutual Information and Capacity

The subtraction $H(X) - H(X|Y)$ is of special significance to the communication problem. Since $H(X)$ is the amount of uncertainty in X before observing Y, this quantity can be interpreted as the reduction in uncertainty of X from the observation of Y. It is the amount of information in Y about X and it is called *mutual information*:

$$I(X;Y) = H(X) - H(X|Y) = H(Y) - H(Y|X) \tag{A.1.7}$$

From the equation (A.1.6) it comes that the mutual information $I(X;Y)$ is a non-negative quantity, and it is equal to zero if X and Y are indipendent.

To decode the transmitted symbol correctly with high probability, it is clear that the mutual information has to be high, *i.e.* $H(X|Y)$ has to be close to zero.

The highest achievable value of the mutual information is called *capacity* of the channel:

$$C = \max_{p_X} I(X;Y) \tag{A.1.8}$$

This value is fundamental to the communication problem: Shannon showed that an error-free communication can happen on a *noisy* channel if the transmission rate remains under C and an efficient coding technique is used. Attempting to communicate at rates above C, makes it impossible to drive the error prob. to zero.

The equation (A.1.8) is valid for a point-to-point communication; how is it extended to the multiuser case? It is possible to define the concept of *capacity region*: this is the set of all combinations $(R_1, R_2, \ldots, R_N)$ such that all the N users can simultaneously communicate without errors (at rates $(R_1, R_2, \ldots, R_N)$). Since the users share the same bandwidth, there is a tradeoff for which if one user wants to communicate at a higher rate, the others must lower their.

An important performance measure for multiuser networks is the *sum-capacity*:

$$C_{sum} = \max_{R_1,\ldots,R_N} \sum_{i=1}^{N} R_i \tag{A.1.9}$$

It is the maximum total throughput that can be achieved in the designed network.

A.1.3 Differential Entropy

For continuos random variable X with a PDF $f_X(x)$, the *differential entropy* is defined as:

$$H(X) = -\int_S f_X(x) \log f_X(x) dx \tag{A.1.10}$$

where S is the support set of the random variable X.

For example, considering an uniform distributed random variable, one has:

$$H(X) = -\int_0^a \frac{1}{a} \log(\frac{1}{a}) dx = \log a \tag{A.1.11}$$

Unlike with discrete variables, *differential entropy* can be negative: for $a < 1$, $\log a < 0$.

For the Gaussian distribution $X \sim N(0, \sigma^2)$ with $f_X(x) = (\sqrt{2\pi\sigma^2})^{-1} \exp(\frac{x^2}{2\sigma^2})$, one has:

$$\begin{aligned} H(X) &= -\int_{-\infty}^{\infty} f_X(x) \log_a f_X(x) dx = \\ &= -\int_{-\infty}^{\infty} f_X(x) (\log_a (\sqrt{2\pi\sigma^2})^{-1} - \frac{x^2}{2\sigma^2} \log_a e) dx = \\ &= \frac{1}{2} \log_a (2\pi\sigma^2) + \frac{\log_a e}{2\sigma^2} E_f[X^2] = \frac{1}{2} \log_a (2\pi e \sigma^2) \end{aligned} \tag{A.1.12}$$

It can be shown that Gaussian distribution maximizes *differential entropy*. $H(X)$ depends on the variance of the distribution, but not on the mean value. In fact, *differential entropy* is *invariant* to translations:

$$H(X + c) = H(X) \tag{A.1.13}$$

where c is a constant term.

The mutual information $I(X;Y)$ between two continuos random variable X and Y is defined as:

$$I(X;Y) = \int f_{X,Y}(x,y) \log \frac{f_{X,Y}(x,y)}{f_X(x) f_Y(y)} dx dy \tag{A.1.14}$$

where $f_{X,Y}(x,y)$ is the *joint density function*.

Mutual information can be evaluated through equation (A.1.7), as in the discrete case. In the continuos case, the *conditional differential entropy* $H(Y|X)$ is defined as:

$$H(Y|X) = -\int f_{X,Y}(x,y) H(Y|X = x) dx dy \tag{A.1.15}$$

Mutual information can also be defined using *relative entropy* or Kullback-Leibler divergence, which is:

$$D(f_X || g_X) = \int f_X(x) \log \frac{f_X(x)}{g_X(x)} dx \tag{A.1.16}$$

which leads to:

$$I(X;Y) = D(f_{X,Y}(x,y) || f_X(x) f_Y(y)) \tag{A.1.17}$$

Certain authors prefer to evaluate mutual information with the above limit, which make just use of PDFs, rather than considering differential entropies.

A.2 MATLAB CODE

In this section, the MATLAB code developed for the simulations is outlined. Due to its length, just few important parts are included here.

Entropy Evaluation

The following code is able to evaluate *entropy* from the random variable Z in input. The code section where a Gaussian Mixture, *i.e.* a weighted sum of Gaussians, is used to estimate the PDF of Z served as a benchmark in the initial steps of the work.

The MATLAB function *trapz*(X, Z) returns the approximate integral of Z via the trapezoidal method, with spacing increment X.

```
% Flavio Maschietti - 15/12/2014
% This function models the stochastic variable in input as a weighted sum
% of gaussians, then it calculates the entropy.
%
% Z = Random variable in input
%
% P_Fit = Mixture Gaussian distribution estimated and obtained
% H = Entropy

function[P_Fit, H, H_R]= Entropy(Z)

GMM = 0;
switch GMM
    case 0
        P_Fit = 0;
        H = 0;
    case 1
        Options = statset('MaxIter', 500);
        % gmdistribution.fit(X, k) uses an Expectation Maximization algorithm to
        % construct an object of the gmdistribution class.
        % This object contains maximum likelihood estimates of the parameters in a
        % Gaussian mixture model with k components for data in the n-by-d matrix X,
        % where n is the number of observations and d is the dimension of the data.
        P_Fit = gmdistribution.fit(Z, 2, 'Options', Options, 'Start', 'randSample',
            'Replicates', 50); % More iterations are concluded to reach convergence

```

```
27          % Extract variance of the Gaussian Mixture distribution
28          varComponents = squeeze(P_Fit.Sigma);
29          % Extract the minimum standard deviation from the variance
30          stdmin = sqrt(min(varComponents));
31          % The minimum is taken because the step of integration must be compatible
32          % with the narrower distribution
33
34          % Considered interval of integration
35          x = (-10*std(Z):stdmin/10:10*std(Z))';
36
37          % Entropy
38          H = - trapz(x, P_Fit.pdf(x).*log(P_Fit.pdf(x))) / log(2);
39  end
40  % Direct calculation of the Entropy from the random variable in input
41  [N_H, X_H] = hist(Z, 250);
42  PDF = N_H / trapz(X_H, N_H);
43  for k = 1:length(PDF)
44      if (PDF(k) == 0)
45          PDF(k) = 1e-6; % To simply avoid numerical instability
46      end
47  end
48  H_R = - trapz(X_H, PDF .* log(PDF)) / log(2);
```

Sync Tool

The following code manages *asynchronization* between users, each signal is oversampled, and then convolved with a Scholz pulse, a usual choice in UWB communications.

Signal-to-Noise ratio is changed after oversampling.

```
% Flavio Maschietti – 23/03/2015
% This function provides a matrix containing K user signals
% which are NOT SYNCHRONIZED. The desynchronization is made possible
% with the generation of (K – 1) time misalignments.

% HYPO: the signals are perfectly sampled, at Nyquist frequency;
% the value in each time bin (Chip) of the DISCRETE time model contains
% the PEAK value of the emitted or replicated (by multipath) waveform
% HYPO: the waveform occupy the entire chip time (Tc = Tm).

function [ Out, Dith, In, SchPulse, OverSam ] = Sync_Tool(In, Chip_Num, IRP)

% Sampling period [s]
SamplingPeriod = 1 / 0.25e2;
% Chip Time [s]
Tc = 1e-9;
% Pulse duration [s]
Tm = Tc;
% Number of samples to represent the pulse
Sampl = floor(Tm / SamplingPeriod);

% Shape factor
Tau = Tm / 2;

% Scholz pulse
if (Sampl == 1)
    T = 0;
else
    T = linspace(-Tm/2, Tm/2, Sampl);
end
Scholtz = (1 - 4.*pi.*((T./Tau).^2)).*exp(-2.*pi.*((T./Tau).^2));
SchPulse = Scholtz / norm(Scholtz);

```

```
% Users
U = size(In, 2);
% (K - 1) Time misalignments (-Tc < Dither < Tc)
Dith = - Chip_Num*Tc + 2*Chip_Num*Tc*rand(1, U); % Misalignent max = Frame time

% Oversampling input matrix
Over_In = upsample(In, Sampl);
% Pulse shaping
Shaped_In = zeros(size(Over_In, 1), U);
for n = 1 : U
    Shaped_In(:, n) = conv(Over_In(:, n), SchPulse, 'same');
end

Shaped_Out = Shaped_In;
for n = 1 : U
    if n == IRP
    else
        % Misalignment index
        IM = round(Sampl*Dith(n));
        Shaped_Out(:, n) = circshift(Shaped_In(:, n), IM);
    end
end

Out = Shaped_Out;
OverSam = Sampl;

end
```

Main script

The following code is the actual simulator. It creates the network scenario and starts the simulation. At the end, results are plotted, although no graphs section is shown here.

```
% Flavio Maschietti – (started on) 11/12/2014
% Main script (Unsynchronized – with INTER-FRAME-SYMBOL Interference)

close all
clear all

% General parameters
Lambda = 1; % Density

Pairs_Edge = 20; % Num. of pairs
U_Edge = Pairs_Edge*2; % Num. of users

Frame_Num = 0.5e4; % Frame number on each attempt

K = Pairs_Edge; % Number of pairs
% (Fixed Load, increasing K leads to have more multi user interference)
Load = 1;
% Number of chips in a frame (Length of spreading sequence)
N = ceil(K ./ Load);

% SNR (Signal Power / SigmaN2)
Gamma_dB = (-20:10:40);
% Gamma_dB = 30;
Gamma = 10.^(Gamma_dB ./ 10);

% Noise variance
SigmaN2 = 1;

Attempts = 0.5e4; % Montecarlo trials
Scenario_Num = 4; % Scenario (receivers) considered

% INITIALIZATIONS
I_YB = zeros(length(N), length(Gamma), Scenario_Num, Attempts);
I_YB_R = zeros(length(N), length(Gamma), Scenario_Num, Attempts);
```

```
35 BitR = zeros(length(N), length(Gamma), Scenario_Num, Attempts);
36 BitR_R = zeros(length(N), length(Gamma), Scenario_Num, Attempts);
37 SpectralE = zeros(length(N), length(Gamma), Scenario_Num, Attempts);
38 SpectralE_R = zeros(length(N), length(Gamma), Scenario_Num, Attempts);
39
40 for m = 1 : Attempts % Montecarlo Loop
41
42   % Topology Generation (R = Node number, 1C = X coord, 2C = Y coord)
43   Pos = Topol_Gen(Lambda, U_Edge);
44   figure(1);
45   scatter(Pos(:,1), Pos(:,2));
46   set(gca, 'FontName', 'Palatino');
47
48   % Pairs definition (R = Pair number, 1C = Tx number, 2C = Rx number)
49   Pairs = Pairs_Gen(U_Edge);
50
51   % Plot paired node TX and RX
52   scatter(Pos(Pairs(:,1), 1), Pos(Pairs(:,1), 2), 36, [0.1 0.1 0.5], ...
53     'd', 'Linewidth', 2);
54   hold on
55   grid on
56   scatter(Pos(Pairs(:,2), 1), Pos(Pairs(:,2), 2), 36, [1 0.45 0.15], ...
57     'o', 'filled', 'Linewidth', 2);
58   axis([0 sqrt(Lambda*U_Edge) 0 sqrt(Lambda*U_Edge)]);
59   set(gca, 'FontName', 'Palatino');
60
61   % Reference pair index
62   IRP = Pairs_Edge;
63
64   % Plot paired node links
65   for p = 1 : length(Pairs)
66     if (p == IRP)
67
68       x = [Pos(Pairs(p,1), 1), Pos(Pairs(p,2), 1)];
69       y = [Pos(Pairs(p,1), 2), Pos(Pairs(p,2), 2)];
70
71       line(x, y, 'Color', [0.4 0.8 0.85], 'Linestyle', '-.');
72
73     else
```

```
74
75          x = [Pos(Pairs(p,1), 1),Pos(Pairs(p,2), 1)];
76          y = [Pos(Pairs(p,1), 2),Pos(Pairs(p,2), 2)];
77
78          line(x, y, 'Color', [0.35 0.55 0.85]);
79
80        end
81      end
82
83      % Definition of the distance between each TX and the reference RX
84      [Distance, Distance_R] = Distance_Calc( Pairs, Pos, IRP );
85
86      % UWB Channel
87      %
88      % Ideal
89      % h_DT = UWB_Discrete_Impulse_Response_Ideal(Pairs_Edge);
90      % Simple Multipath
91      % h_DT = UWB_Discrete_Impulse_Response_Simple_Multipath(Pairs_Edge);
92      % 802.15.3a Model
93      h_DT = UWB_Discrete_Impulse_Response_802_15_3a(Pairs_Edge);
94      h_DT_Inv = zeros(50, 1);
95
96      for q = 1 : Scenario_Num % Scenario Loop
97
98        % AllRake and Precoding (Time Reversal) activators (boolean)
99        if (q == 1)
100         AllRake = 0; % Deactivate to obtain NRake receiver
101         PreCod = 1;
102         % Activate to base Time Reversal on the channel between
103         % the reference receiver and each other transmitter
104         TR_Mod = 0;
105         TR_Mean = 0;
106       end
107       if (q == 2)
108         AllRake = 1; % Activate to obtain AllRake receiver w/ Time Reversal
109         PreCod = 1;
110         TR_Mod = 0; % With TR_Mod = 0, TimeReversal is based on each pair channel
111         TR_Mean = 0; % Time Reversal is made on a mean basis
112       end
```

```
113     if (q == 3)
114       AllRake = 0; % Activate to obtain AllRake receiver w/ Time Reversal
115       PreCod = 0;
116       TR_Mod = 0; % With TR_Mod = 0, TimeReversal is based on each pair channel
117       TR_Mean = 0; % Time Reversal is made on a mean basis
118     end
119     if (q == 4)
120       AllRake = 1; % Activate to obtain AllRake receiver w/ Time Reversal
121       PreCod = 0;
122       TR_Mod = 0; % With TR_Mod = 0, TimeReversal is based on each pair channel
123       TR_Mean = 0; % Time Reversal is made on a mean basis
124     end
125
126     for t = 1 : length(N) % Load Loop
127
128       for p = 1 : length(Gamma) % SNR Loop
129
130         disp('Remaining:');
131         disp([' ', num2str(Attempts - m) , '.', ...
132           num2str(Scenario_Num - q), '.', ...
133           num2str(length(N) - t), '.', num2str(length(Gamma) - p)]);
134         Z = zeros(Frame_Num, 1);
135         b_Z = zeros(Frame_Num, 1);
136         D = zeros(150+(Frame_Num*N(t)), K);
137
138         for k = 1 : K % User Loop
139
140           if (PreCod == 1)
141             % w/ Precoding
142             Tau = 0;
143             % (Tau = 0, perfect channel state informations;
144             % Tau > 0, imperfect channel state informations)
145             if (TR_Mod == 1)
146               h_DT_Inv = (flipud(sqrt(1-Tau^2)*h_DT(:, k, IRP) + ...
147                 Tau*randn(length(h_DT(:, k, IRP)), 1))) / ...
148                 norm(h_DT(:, k, IRP)); % Normalized because of power constraint
149             else h_DT_Inv = (flipud(sqrt(1-Tau^2)*h_DT(:, k, k) + ...
150                 Tau*randn(length(h_DT(:, k, k)), 1))) / ...
151                 norm(h_DT(:, k, k));
```

```
152             end
153             if (TR_Mean == 1)
154               h_DT_Inv_M = zeros(50, 1);
155               for v = 1 : K
156                 h_DT_Inv_M = h_DT_Inv_M + ( (flipud(sqrt(1-Tau^2)*h_DT(:, k, v) + ...
157                   Tau*randn(length(h_DT(:, k, v)), 1))) / ...
158                   norm(h_DT(:, k, v)) );
159               end
160               h_DT_Inv_M = (h_DT_Inv_M * pinv(K));
161               h_DT_Inv = h_DT_Inv_M / norm(h_DT_Inv_M);
162             end
163             % Inverted IR adjustment
164             Shift = 50 - (find(h_DT_Inv, 1) - 1);
165             h_DT_Inv = circshift(h_DT_Inv, Shift);
166             % TR adjustment
167             L = length(h_DT_Inv);
168             % Precoding matrix for pair k
169             P = convmtx(h_DT_Inv, N(t)+L);
170             % Channel matrix for pair k
171             C = convmtx(h_DT(:, k, IRP) / norm(h_DT(:, k, IRP)), N(t)+(2*L)-1);
172           else
173             % w/o Precoding
174             % Channel matrix (Convolutional matrix) for pair k
175             C = convmtx(h_DT(:, k, IRP) / norm(h_DT(:, k, IRP)), N(t));
176             % TR adjustment
177             L = 0;
178             % Precoding matrix for pair k
179             P = eye(N(t));
180           end
181
182           for d = 1 : Frame_Num % Frame Loop
183
184             % Transmitter chain
185             b = sqrt(Gamma(p)*SigmaN2*N(t))*(randn); % Symbol to transmit
186             % A Time Hopping vector is generated for each pair
187             S_TH = TH_Code_Gen(N(t), L);
188             x = S_TH * b; % The symbol is assigned to one chip between N
189             % The symbol is transmitted with possible Precoding
190             x_Tx = P * x;
```

```
191
192             % The symbol arrives to the reference RX
193             % (with eventual propagation effects)
194             y = C * (sqrt(Distance_R(k)^(-2)) * x_Tx);
195
196             % Saving the reference communication
197             if (k == IRP)
198               y_R(1+(length(y)*(d - 1)):(length(y)*d), 1) = y;
199               TH_R(1+(length(S_TH)*(d - 1)):(length(S_TH)*d), 1) = S_TH;
200               C_R = C;
201               % The Precoding matrix is estimated by the receiver
202               % with the same estimation error Tau
203               if (PreCod == 1)
204                 h_DT_Inv = (flipud(sqrt(1-Tau^2)*h_DT(:, k, IRP) + ...
205                   Tau*randn(length(h_DT(:, k, IRP)), 1))) / ...
206                    norm(h_DT(:, k, IRP));
207                 h_DT_Inv = circshift(h_DT_Inv, Shift);
208                 P_R = convmtx(h_DT_Inv, N(t)+L);
209               end
210             end
211
212             % Saving data to sum
213             D(1+(N(t)*(d - 1)):(length(y)+(d - 1)*N(t)), k) = ...
214               D(1+(N(t)*(d - 1)):(length(y)+(d - 1)*N(t)), k) + y;
215
216           end
217
218         end
219
220         % Synchronization removal
221         [D, Dith, D_Pre, Pulse, OverSampl] = Sync_Tool(D, N(t), IRP);
222
223         % Thermal noise with variance SigmaN2 is added
224         D = D + sqrt(SigmaN2)*randn(size(D));
225
226         % Oversampling and shaping of the reference signal
227         Over_y_R = upsample(y_R, OverSampl);
228         Shaped_y_R = conv(Over_y_R, Pulse, 'same');
229
```

```
230         for d = 1 : Frame_Num
231
232           % Frame arrived to the reference RX
233           y_k_Rx = sum(D(1+(N(t)*(d - 1)*OverSampl): ...
234             ((length(y)+(d - 1)*N(t))*OverSampl), :), 2);
235           % The reference signal is subtracted
236           y_Z = y_k_Rx - Shaped_y_R(1+(length(y)*(d - 1)*OverSampl): ...
237             (length(y)*d*OverSampl));
238           % Computation of the interference decision variable
239           if (PreCod == 1)
240             % AllRake receiver
241             M = C_R * P_R * TH_R(1+(length(S_TH)*(d - 1)):(length(S_TH)*d));
242             if (AllRake == 0)
243               % 1Rake receiver
244               [TR_Max, TR_Ind] = max(abs(M));
245               Temp = zeros(length(M), 1);
246               Temp(TR_Ind) = M(TR_Ind);
247               M = Temp;
248             end
249             Over_M = upsample(M, OverSampl);
250             Shaped_M = conv(Over_M, Pulse, 'same');
251             Z(d, 1) = (Shaped_M)' * y_Z * pinv(norm(Shaped_M));
252             b_Z(d, 1) = (Shaped_M)' * ...
253               Shaped_y_R(1+(length(y)*(d - 1)*OverSampl):...
254               (length(y)*d*OverSampl)) * ...
255               pinv(norm(Shaped_M));
256           else
257             % AllRake receiver
258             M = C_R * TH_R(1+(length(S_TH)*(d - 1)):(length(S_TH)*d));
259             if (AllRake == 0)
260               % 1Rake receiver
261               [TR_Max, TR_Ind] = max(abs(M));
262               Temp = zeros(length(M), 1);
263               Temp(TR_Ind) = M(TR_Ind);
264               M = Temp;
265             end
266             Over_M = upsample(M, OverSampl);
267             Shaped_M = conv(Over_M, Pulse, 'same');
268             Z(d, 1) = (Shaped_M)' * y_Z * pinv(norm(Shaped_M));
```

```
269             b_Z(d, 1) = (Shaped_M)' * ...
270               Shaped_y_R(1+(length(y)*(d - 1)*OverSampl):...
271               (length(y)*d*OverSampl)) * ...
272               pinv(norm(Shaped_M));
273             % Decorrelator receiver
274             % Z(d, 1) = pinv(Shaped_M) * y_Z;
275             % MMSE receiver
276             % W = ((M' * M) + ((Gamma(p)^(-1))*eye(size(M' * M))))^(-1) * M';
277             % Z(d, 1) = W * y_Z;
278
279           end
280
281         end
282
283         % Interference and output variable
284         ZE = Z;
285         Y = ZE + b_Z;
286
287         % Entropy evaluation
288         [P_ZE, h_ZE, h_ZE_R] = Entropy(ZE);
289         [P_Y, h_Y, h_Y_R] = Entropy(Y);
290
291         % Mutual Information obtained from Gaussian Mixture estimation
292         I_YB(t, p, q, m) = h_Y - h_ZE;
293         % Mutual information obtained directly from Z values
294         I_YB_R(t, p, q, m) = h_Y_R - h_ZE_R;
295
296         % BitRate obtained from Gaussian Mixture estimation
297         BitR(t, p, q, m) = I_YB(t, p, q, m) * pinv(N(t)) * K * Tc;
298         % BitRate obtained directly from Z values
299         BitR_R(t, p, q, m) = I_YB_R(t, p, q, m) * pinv(N(t)) * K * Tc;
300
301         % Spectral Efficiency obtained from Gaussian Mixture estimation
302         SpectralE(t, p, q, m) = I_YB(t, p, q, m) * pinv(N(t)) * K;
303         % Spectral Efficiency obtained directly from Z values
304         SpectralE_R(t, p, q, m) = I_YB_R(t, p, q, m) * pinv(N(t)) * K;
305
306       end
307
```

```
308         end
309
310     end
311
312 end
313
314 % Mean value
315 I_YB = mean(I_YB, 4);
316 I_YB_R = mean(I_YB_R, 4);
317 BitR = mean(BitR, 4);
318 BitR_R = mean(BitR_R, 4);
319 SpectralE = mean(SpectralE, 4);
320 SpectralE_R = mean(SpectralE_R, 4);
```

B BIBLIOGRAPHY

Beaulieu, Norman C. and David J. Young

2009 *Designing Time-Hopping UWB Receivers for Multiuser Interference Environments*, IEEE Proceedings.

Chiani, Marco

1997 *Introducing erasures in decision-feedback equalization to reduce error propagation*, IEEE Transactions on Communications, vol. 45. (Cited on p. 45.)

Chung, Gwo C., Mohamad Y. Alias, and Teong C. Chuah

2007 *An adaptive minimum bit-error decision-feedback equalizer for UWB systems*, IEICE Electron. Express. (Cited on p. 45.)

Deleuze, Anne-Laure, Philippe Ciblat, and Christophe J. Le Martret

2005 *Inter-symbol / inter-frame interference in time-hopping ultra wideband impulse radio system*, IEEE International Conference on Ultra-Wideband. (Cited on pp. 11, 12.)

Di Benedetto, Maria-Gabriella and Guerino Giancola

2004 *Understanding Ultra Wide Band Radio Fundamentals*, Prentice Hall.

Di Benedetto, Maria-Gabriella, Thomas Kaiser, Andreas F. Molish, and Ian Oppermann

2006 *UWB Communication Systems: A Comprehensive Overview*, Hindawi Publishing Corporation.

Emami, Shahriar

2013 *UWB Communication Systems: Conventional and 60GHz*, Springer.

Eslami, Mohsen and Xiaodai Dong

2005 *Rake-MMSE equalizer performance for UWB*, IEEE Communications Letters. (Cited on p. 44.)

Ferrante, Guido Carlo

2015 *Shaping Interference Towards Optimality of Modern Wireless Communication Transceivers*, PhD thesis, La Sapienza, University of Rome and CentraleSupélec. (Cited on p. 12.)

Ferrante, Guido Carlo, Yassin Elhillali, Maria-Gabriella Di Benedetto, Fouzia E. Boukour, and Atika Rivenq

2013 *Experimental acquisition of UWB channel impulse responses*, COST Action IC0902, Cognitive Radio and Networking for Cooperative Coexistence of Heterogeneous Wireless Networks. (Cited on p. 41.)

Ferrante, Guido Carlo, Jocelyn Fiorina, and Maria-Gabriella Di Benedetto

2014 *Time Reversal Beamforming in MISO-UWB Channels*, IEEE International Conference on Ultra-Wideband.

Fiorina, Jocelyn, Guido Capodanno, and Maria-Gabriella Di Benedetto

2011 *Impact of Time Reversal on multi-user interference in IR-UWB*, IEEE International Conference on Ultra-Wideband. (Cited on p. 11.)

Foerster, Jeffrey R., Marcus Pendergrass, and Andreas F. Molisch

2003 *A Channel Model for Ultrawideband Indoor Communication*, Proceedings of International Symposium on Wireless Personal Multimedia Communication.

Ghavami, Mohammad and Lachlan Michael

2004 *Ultra Wideband Signals and Systems in Communication Engineering*, Wiley.

Giancola, Guerino, Luca De Nardis, and Maria-Gabriella Di Benedetto

2003 *Multiuser interference in power-unbalanced ultra wide band systems: analysis and verification*, IEEE Conference on Ultra Wideband Systems and Technologies. (Cited on pp. 11, 12.)

Li, Y and Andreas F. Molisch

2003 *Channel Estimation and Signal Detection for UWB*.

Lopez-Salcedo, Jose

2007 *Coherent and Non-Coherent UWB Communications*, PhD thesis, UPC.

Molisch, Andreas F.

2005 *Wireless Communications*, IEEE Press.

2008 *Ultrawideband Communications - An Overview*.

Oppenheim, Alan V. and Ronald W. Schafer

2009 *Discrete-Time Signal Processing*, 3rd, Prentice Hall Press.

Panaitopol, Dorin

2011 *Ultra Wide Band Ad-Hoc Sensor Networks: a Multi-Layer Analysis*, PhD thesis, Supélec and National University of Singapore. (Cited on pp. 11, 12.)

Popovski, Keni, Beata J. Wisocki, and Tadeusz A. Wisocki

2007 *Modelling and Comparative Performance Analysis of a Time-Reversed UWB System*, EURASIP Journal on Wireless Communications and Networking. (Cited on p. 11.)

Proakis, John G. and Masoud Salehi

2008 *Digital Communications*, McGraw-Hill.

Reuter, Michael, J. C. Allen, James R. Zeidler, and Richard C. North

2001 *Mitigating error propagation effects in a decision feedback equalizer*, IEEE Transactions on Communications.

Tse, David and Pramod Viswanath

2005 *Fundamentals of Wireless Communications*, Cambridge University Press.